MICHIGAN SCIENTIFIC
corporation

AN INVESTIGATION OF DRIVELINE INCIDENTS OF THE US ARMY'S MODEL M1078 LIGHT MEDIUM TACTICAL VEHICLE (LMTV)

This report covers work performed from April 1998 through December 1998

REQUESTED BY:

US ARMY TANK-AUTOMOTIVE AND ARMAMENTS COMMAND (TACOM)

CONTRACT NUMBER:

DAAE07-98-C-M012

DISTRIBUTION STATEMENT A
Approved for Public Release
Distribution Unlimited

Michigan Scientific Corporation • 321 East Huron Street • Milford, MI 48381
Telephone: 248-685-3939 • FAX: 248-684-5406

710 035

REPORT DOCUMENTATION PAGE	Form Approved OMB No. 0704-0188

1. REPORT DATE *(DD-MM-YYYY)*	2. REPORT TYPE	3. DATES COVERED *(From - To)*
28-02-2003	A005 DATA ITEM	01-04-1998 TO 28-02-2003

4. TITLE AND SUBTITLE

FINAL REPORT for Contract DAAE07-98-C-M012 (PART 2 OF 3)
-An Investigation of Driveline Incidents of the US Army's Model 1078 Light Medium Tactical Vehicle (LMTV)

5a. CONTRACT NUMBER
DAAE07-98-C-M012

5b. GRANT NUMBER

5c. PROGRAM ELEMENT NUMBER

6. AUTHOR(S)
-HAYES HOBOLTH
-HUGH LARSEN
-ED MCLENON
-ROBERT WASHNOCK

5d. PROJECT NUMBER

5e.

5f.

20030710 035

7. PERFORMING ORGANIZATION NAME(S) AND ADDRESS(ES)
MICHIGAN SCIENTIFIC CORPORATION
730 BELLEVUE AVENUE
MILFORD, MI 48381

8. PERFORMING ORGANIZATION REPORT NUMBER
A005

9. SPONSORING/MONITORING AGENCY NAME(S) AND ADDRESS(ES)
UNITED STATES ARMY- TACOM
WARREN, MI 48397-5000
JAMES YAKEL, COTR

10. SPONSOR/MONITOR'S ACRONYM(S)
N/A

11. SPONSOR/MONITOR'S REPORT NUMBER(S)
N/A

12. DISTRIBUTION/AVAILABILITY STATEMENT

DISTRIBUTION STATEMENT A

13. SUPPLEMENTARY NOTES
TEXT DOCUMENT LOCATED ON CD (A) IN MICROSOFT WORD FORMAT

14. ABSTRACT

ROOT CAUSE ANALYSIS AND DEVELOPMENT OF RECOMMENDED CORRECTIVE ACTIONS FOR CRACKED FLYWHEEL HOUSINGS AND DRIVESHAFT UNIVERSAL JOINT FAILURES IN MODEL M1078 2 1/2 TON LIGHT MEDIUM TACTICAL VEHICLE 4X4 TRUCKS ARE THE PRIMARY FOCUS OF THIS REPORT. THE COMPLEX DYNAMIC SYSYTEM REQUIRED SPECIALIZED INSTRUMENTATION AND MATHEMATICAL MODELING TO HELP UNDERSTAND THE PROBLEM AND PRESCRIBE CORRECTIVE ACTIONS. THIS REPORT DETAILS THE ENGINEERING INVESTIGATION CONDUCTED BY MICHIGAN SCIENTIFIC CORPORATION (MSC) AND INDEPENDENTLY BY DR. JOHN F. MARTIN OF MICHIGAN STATE UNIVERSITY DURING THE MONTHS OF APRIL 1998 THROUGH DECEMBER 1998.

15. SUBJECT TERMS

FMTV, LMTV, DRIVESHAFT, CARDAN, CV, CONSTANT VELOCITY, FLYWHEEL HOUSING, BELL HOUSING, CRITICAL SPEED, DRIVELINE, DRIVELINE DYNAMICS, DRIVELINE MODEL, POWERPACK, POWERPACK DYNAMICS, TRANSFER CASE TRANSDUCER, DRIVESHAFT BALANCE, DADS MODEL.

16. SECURITY CLASSIFICATION OF:			17. LIMITATION OF ABSTRACT	18. NUMBER OF PAGES	19a. NAME OF RESPONSIBLE PERSON
a. REPORT	b. ABSTRACT	c. THIS PAGE			HAYES HOBOLTH
UNCLASS	UNCLASS	UNCLASS	UNCLASS	60	19b. TELEPHONE NUMBER *(Include area code)* 248-685-3939

MICHIGAN SCIENTIFIC
corporation

ENGINEERING REPORT

Requested By: US Army Tank-Automotive and Armaments Command (TACOM), Contract #DAAE07-98-C-M012

Michigan Scientific Corporation Project Code: TACOM-FMTV

Date: March 3, 1999

Title: An Investigation of Driveline Incidents of the US Army's Model M1078 Light Medium Tactical Vehicle (LMTV)

Abstract: Root cause analysis and development of recommended corrective actions for cracked flywheel housings and driveshaft universal joint failures in model M1078 2½ ton Light Medium Tactical Vehicle 4X4 trucks are the primary focus of this report. The complex dynamic system required specialized instrumentation and mathematical modeling to help understand the problem and prescribe corrective actions. This report details the engineering investigation conducted by Michigan Scientific Corporation (MSC) and independently by Dr. John F. Martin of Michigan State University during the months of April 1998 through December 1998.

Distribution: TACOM
Michigan Scientific Corp.
Dr. John F. Martin

Author: _____
Hayes M. Hobolth

Author: _____
Edward J. Mclenon

Author: _____
Robert J. Washnock

Approved: _____
Hugh W. Larsen

Michigan Scientific Corporation • 321 East Huron Street • Milford, MI 48381
Telephone: 248-685-3939 • FAX: 248-684-5406

MICHIGAN SCIENTIFIC
corporation

ENGINEERING REPORT

Requested By: US Army Tank-Automotive and Armaments Command (TACOM), Contract #DAAE07-98-M012

Michigan Scientific Corporation Project Code: TACOM-FMTV

Date: March 3, 1999

Title: An Investigation of Driveline Incidents of the US Army's Model M1078 Light Medium Tactical Vehicle (LMTV)

Abstract: Root cause analysis and development of recommended corrective actions for cracked flywheel housings and driveshaft universal joint failures in model M1078 2½ ton Light Medium Tactical Vehicle 4X4 trucks are the primary focus of this report. The complex dynamic system required specialized instrumentation and mathematical modeling to help understand the problem and prescribe corrective actions. This report details the engineering investigation conducted by Michigan Scientific Corporation (MSC) and independently by Dr. John F. Martin of Michigan State University during the months of April 1998 through December 1998.

Distribution: TACOM
Michigan Scientific Corp.
Dr. John F. Martin

Author: Hayes M. Hobolth
Hayes M. Hobolth

Author: Edward J. McLenon
Edward J. Mclenon

Author: Robert J. Washnock
Robert J. Washnock

Approved: Hugh W. Larsen
Hugh W. Larsen

Michigan Scientific Corporation • 321 East Huron Street • Milford, MI 48381
Telephone: 248-685-3939 • FAX: 248-684-5406

TABLE OF CONTENTS

List of Figures iv

1. Introduction 1

2. Overall Results and Conclusions

    2.1 Identification of the Root Cause of the Problem 2

    2.2 Secondary Causes 7

3. Recommendations 8

4. Overview of Project

    4.1 Description of the Failures 9

    4.2 Summary of Testing 10

    4.3 Driveshaft Design Features 12

5. Computer Model of LMTV Driveline Dynamics

    5.1 Model Description 13

    5.2 Model Construction 13

    5.3 Spring Rates, Inertias, and Damping 14

    5.4 Limitations of the Model 16

    5.5 Assumptions 17

    5.6 Model Validation 17

    5.7 Driveshafts Modeled

        5.7.1 Meritor Original Production Driveshaft 17

        5.7.2 MSC Proof of Principle Driveshaft 18

        5.7.3 Proposed Driveshafts 19

        5.7.4 Instrumented Meritor Original Production Driveshaft 22

6. Experimental Measurements of Rear Driveshaft Dynamics

    6.1 Introduction 28

    6.2 Results 29

    6.3 Measurement Methodology 29

6.4 Instrumentation 31

6.5 Presentation and Analysis of the Experimental Data 32

Appendix A: Experimental Measurement of Lateral and Vertical Powerpack Bending Stiffness

Appendix B: Experimental Meas. of Driveshaft Hinge Stiffness for Meritor "Orig. Production" & "A1" Driveshafts

Appendix C: Pre and Post Test Instrumented Driveshaft Total Indicated Run-Out Measurements

Appendix D: Transfer Case Rear Output Yoke Stiffness Measurement

Appendix E: Index of Datasets Pertinent to Instrumented Driveshaft Measurements

Appendix F: Transfer Functions of Anti-Alias Filters Used in the Digital Data Acquisition

Appendix G: Pre Test Spline Lash Hinge Measurement

Appendix H: Simplified Mechanical Model, by Dr. John F. Martin, Michigan State University

Separate Supplementary Material: *Experimental Data Appendix to Master Report, Volumes 1, 2, 3, & 4*

LIST OF FIGURES

Figure 1.1 Illustrations of M1078 LMTV cargo truck 1

Figure 2.1 Illustration of powerpack configuration 2

Figure 2.2 Flywheel housing strain as excited by both the T-C driveshaft components and the eng/trans 3-4

Figure 2.3 Photograph of strain gage "GAGE #1" on CAT original flywheel housing 5

Figure 2.4 Waterfall plot showing relative amplitudes of T-C driveshaft components and eng/trans excitation 5

Figure 2.5 Strain at GAGE #1, torque converter locked, lockup "A" 6

Figure 2.6 Strain at GAGE #1, torque converter locked, lockup "B" 6

Figure 2.7 Strain at GAGE #1, torque converter unlocked 7

Figure 2.7 Photograph of welding of thrust washer to cross of front U-joint of rear driveshaft 8

Figure 4.1 Photograph of typical flywheel housing crack 9

Figure 4.2 Photograph of failure of front U-joint of rear driveshaft 10

Figure 4.3 Bending mode shape of powerpack 11

Figure 4.4 Comparison of flywheel housing stiffnesses, original vs MSC design 12

Figure 5.1 MSC DADS model configuration 13

Figure 5.2 MSC DADS model configuration showing spring locations 15

Figure 5.3 MSC DADS model configuration showing inertia locations 16

Figure 5.4 Meritor ADAMS model of original production driveshaft 17

Figure 5.5 MSC DADS model output of Meritor original production driveshaft 18

Figure 5.6 Photograph MSC proof of principle driveshaft 19

Figure 5.7 MSC DADS model output of MSC proof of principle driveshaft 19

Figure 5.8 MSC DADS model output of Meritor interim driveshaft with orig. driveshaft hinge stiffness used 20

Figure 5.9 MSC DADS model output of Meritor A1 driveshaft with A1 measured hinge stiffness used 20

Figure 5.10 Flywheel housing strain data with Meritor A1 driveshaft 21

Figure 5.11 MSC revised design driveshaft 22

Figure 5.12 MSC DADS model output of MSC revised driveshaft 22

Figure 5.13 Photograph of instrumented Meritor original production driveshaft 23

Figures 5.14 Model data vs experimental data for U-joint force of rear driveshaft 24

Figures 5.15 Data of figure 5.15 with rescaled time axis 25-26

Figure 5.16 MSC DADS model output of instrumented Meritor original production driveshaft 27

Figure 6.1 Illustration of M1078 LMTV cargo truck (Figure 1.1 repeated) 28

Figure 6.2 Photographs of instrumented Meritor original production driveshaft 30

Figures 6.3 to 6.12 Time history data from instrumented Meritor original production driveshaft 33-37

Figure 6.13 Manipulation algorithm to transform data from rotating to stationary coordinate system 38

Figures 6.14 to 6.18 Time history data from Meritor orig. fact. instr. driveshaft in stationary coord. sys. 39-41

Figure 6.19 "XY" plot of U-joint force data transformed into stationary coordinates 41

1. INTRODUCTION

In April of 1998, the U.S. Department of the Army awarded Michigan Scientific Corporation (MSC) contract number DAAE07-98-C-M012. The stated requirement of the contract was "to determine the cause of driveline and flywheel housing failures in the Light Medium Tactical Vehicle (LMTV) cargo vehicle and develop recommended corrective actions."

By early 1998 the number of field incidents involving failed driveshafts and/or flywheel housings were accumulating at an unacceptable rate. In some incidents the rear driveshafts were thrown from the vehicle. This resulted in the issuance of a Safety Of Use Message (SOUM) limiting the maximum allowable speed of all variants of Family of Medium Tactical Vehicles (FMTV) trucks to 30 mph.

This report covers the investigations by Michigan Scientific Corporation to identify root causes of driveline and flywheel housing failures in the model M1078, 2-½ ton LMTV cargo vehicle and to recommend corrective actions to avoid failures of these components. Illustrations of this vehicle are shown in figure 1.1.

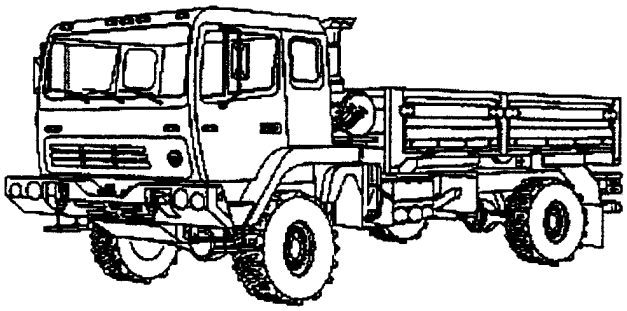

LEFT FRONT VIEW

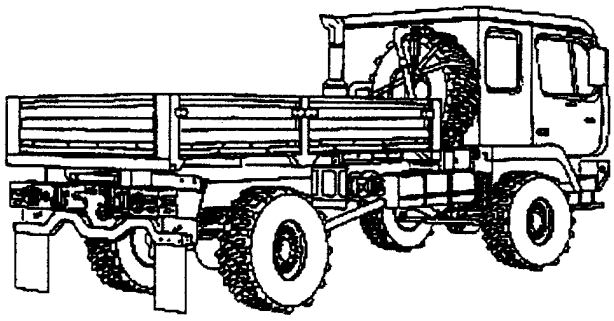

RIGHT REAR VIEW

Figure 1.1 Illustrations of M1078 2½ ton, 4X4, dropside, LMTV cargo truck

2. OVERALL RESULTS AND CONCLUSIONS

2.1 Identification of the Root Cause of the Problem

The M1078 LMTV powertrain has two major resonant responses that are active within the normal driving speed of the vehicle: 1) **powerpack vertical bending** and 2) **driveshaft bending**.

1) **Powerpack vertical bending:** The powerpack vertical bending resonant frequency is lower than a normal powerpack. The low frequency is primarily a result of an integral transmission/transfer case configuration joined to an engine of about equal mass by a relatively elastic flywheel housing (see figure 2.1). This results in a vertical bending resonant frequency of 43 to 48 Hz which corresponds to a 1st order driveshaft speed equivalent to about 44 to 49 mph road speed, a very common operating speed. Also, the same resonant response is excited at level road maximum vehicle speed (55 to 58 mph) by components rotating at engine speed.

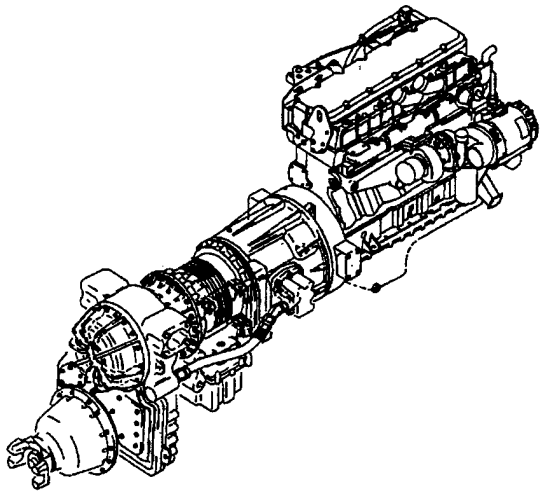

Figure 2.1 Illustration of powerpack configuration

The original housing was made of cast gray iron and the shape allowed some diaphragming action as it was exercised by the bending of the powerpack. MSC revised the shape of the housing to improve the resistance to bending and had experimental housings cast from nodular iron which is stiffer and stronger than gray iron. Caterpillar slightly modified the MSC design to simplify fabrication. Both the MSC nodular iron flywheel housing and the Caterpillar modified version (CAT 2) approximately double the vertical bending resonant frequency.

It is important to note that the powerpack configuration is sensitive to two exciters of differing frequencies: i) the driveshaft and/or components rotating with the driveshaft and ii) the engine/transmission. In seventh gear the engine rotates at 78 percent of the driveshaft speed. In sixth gear the engine rotates at 90 percent driveshaft speed. Figure 2.2 are time history plots of strain at GAGE #1 in gears one through seven (see figure 2.3 for the location of GAGE #1). All of these plots are with *no driveshafts installed.* The plots therefore demonstrate the sensitivity of the powerpack to excitement from components inside the transfer case (including the yokes) that rotate at driveshaft speed. The sixth gear plot clearly shows the presence of both exciting frequencies as indicated by the beating that modulates the amplitude of flywheel housing strain by nearly 100 percent. This amount of modulation implies that the two exciters (in this case transfer case components and engine/transmission components) are nearly equal *in their effect, i.e.* they can be of different magnitudes but affect the system differently because they act at locations of differing sensitivities or driving point mobilities. Figure 2.4 shows a comparison of the two exciters (again, transfer case components and engine/transmission components) in a waterfall plot format during sixth gear operation.

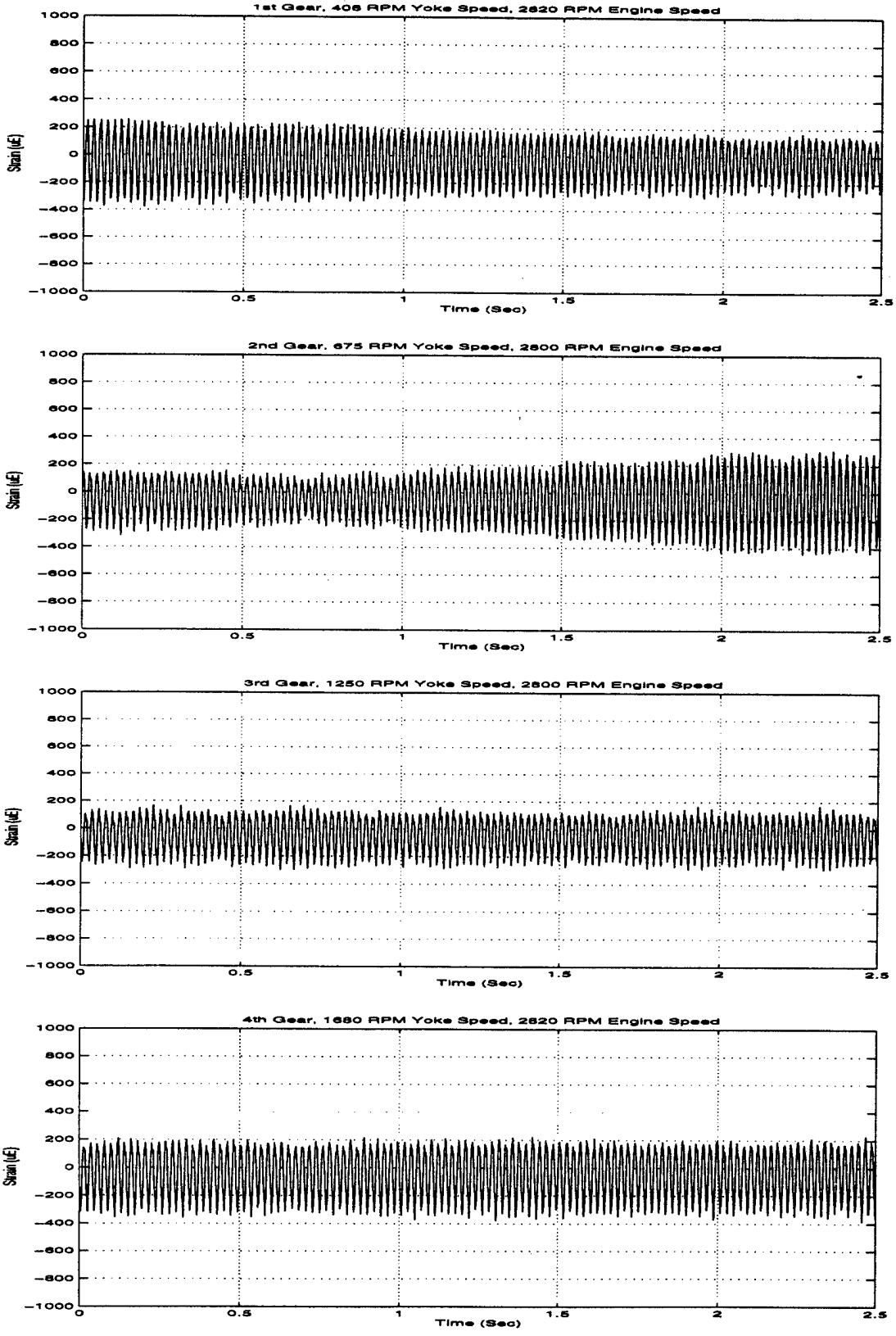

Figure 2.2 Flywheel housing strain at "GAGE #1 as excited by both the transfer case driveshaft components and the engine/transmission components (no driveshafts installed)

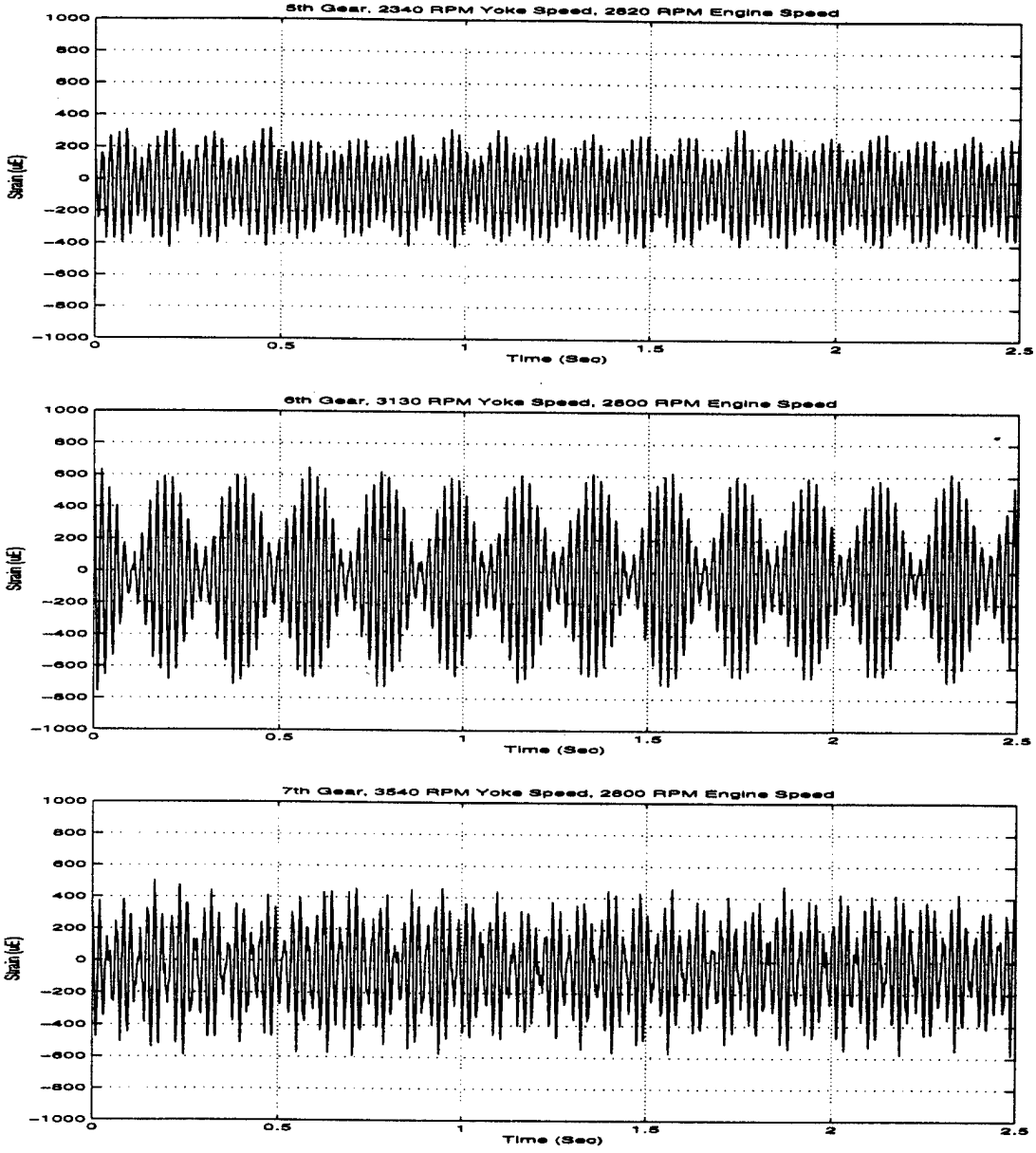

Figure 2.2 (continued) Flywheel housing strain at "GAGE #1 as excited by both the transfer case driveshaft components and the engine/transmission components (no driveshafts installed)

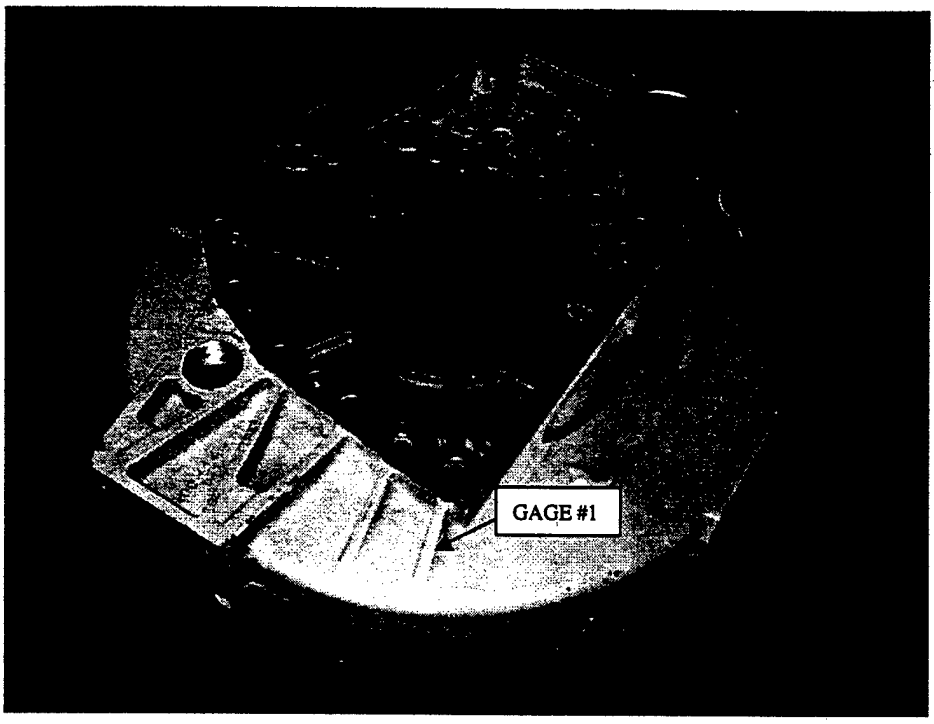

Figure 2.3 Photograph of original CAT flywheel housing gage location #1(engine side shown)

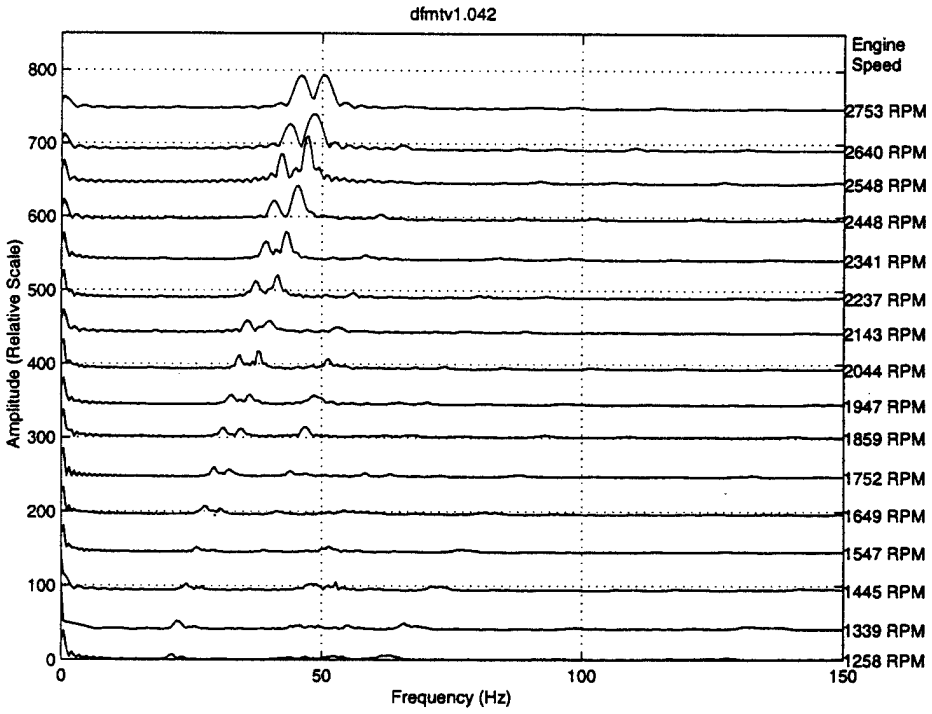

Figure 2.4 Waterfall plot showing relative amplitudes of engine/transmission and driveshaft excitation frequencies during an engine speed sweep in 6th gear (no driveshafts installed)

A major contributor of excitation from the engine/transmission is the torque converter turbine. Its effect was explored by making test runs in neutral with the torque converter clutch locked and unlocked. These results are shown in figures 2.5, 2.6, (two locked up runs: A & B) and 2.7 (one unlocked run). The effect is significant because the resultant force acts near an antinode of the responding system i.e. high driving point mobility. On some early production trucks, the engine cooling fan mounting was also a source of significant excitation.

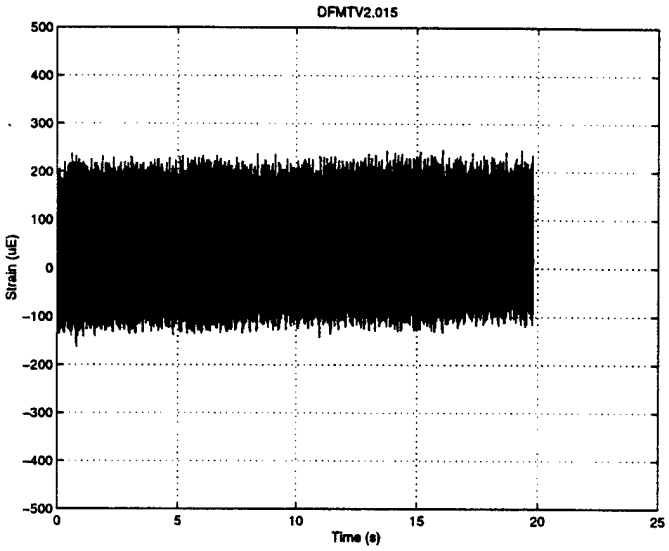

Figure 2.5 Strain sensed at "GAGE #1" (original CAT flywheel housing), no driveshafts, no added unbalance, neutral gear, maximum engine speed, *TORQUE CONVERTER LOCKED, LOCKUP A*

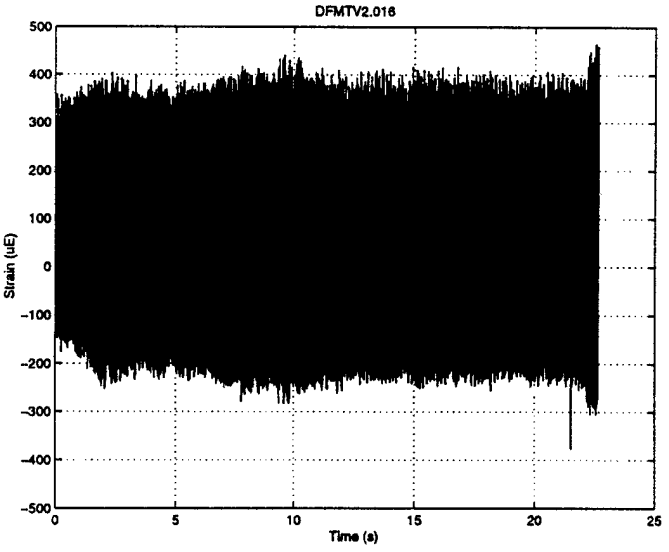

Figure 2.6 Strain sensed at "GAGE #1" (original CAT flywheel housing), no driveshafts, no added unbalance, neutral gear, maximum engine speed, *TORQUE CONVERTER LOCKED, LOCKUP B*

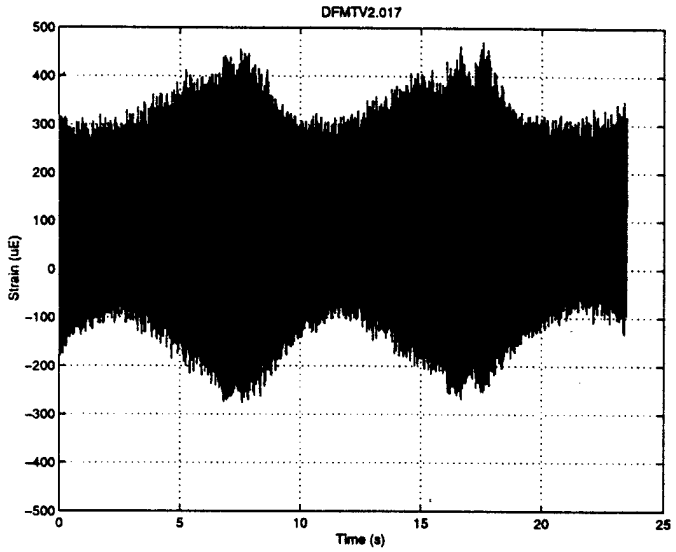

Figure 2.7 Strain sensed at "GAGE #1", no driveshafts, no added unbalance, neutral gear, maximum engine speed, *TORQUE CONVERTER UNLOCKED*

2) **Driveshaft bending:** As the speed of a shaft increases from zero, the speed at which the bending stiffness of the shaft is no longer sufficient to limit the bending caused by centrifugal forces is known as the *critical speed* and is given in revolutions per second or Hertz (Hz). The centrifugal forces are caused by shaft unbalance i.e. when the center of mass does not coincide with the center of rotation: this is virtually always the case with rotating shafts in general. At or near critical speed, shaft deflection is often large enough to break the shaft or produce destructive bearing loads. The critical speed of the Meritor original production rear driveshaft is approximately 66 Hz or only about 17 percent above the driveshaft speed corresponding to the 55 to 58 mph level road maximum speed of the LMTV. For medium size trucks, the Society of Automotive Engineers (SAE) recommends that the maximum operating driveshaft speed be equal or less than 75 percent of the driveshaft critical speed, or in other words, the critical speed of the driveshaft should be greater than 33 percent of the maximum driveshaft speed. At high speed the driveshaft bends significantly adding to the centrifugal force due to static unbalance. This effect compounds exponentially with increasing speed to produce premature failures of either or both types described in section 4.1

2.2 Secondary Causes

The universal joint angles in the LMTV are outside the normal design envelopes for single-cardan universal joints that must operate at the speeds required by the mission profile. The computer model and experimental measurements show that the maximum radial force that must be sustained by the joints can be as high as 1000 lbs. At high speed, the combination of the high radial force and the twice per revolution oscillation can cause localized heating sufficient to break down the lubricant and weld the thrust washer to the cross (see figure 2.8). The "easy service" feature, which uses a strap to retain the bearing cap in the yoke, may contribute to the heating by virtue of deformation of the cap and the reduced heat sinking capabilities. The replacement of the strap by the "full-round" design of the Meritor A1 driveshaft and the replacement of the steel thrust washer by the nylon thrust washer alleviates this heating problem and improves the joint life. It appears that the single-cardan joint may adequately meet the requirements of the LMTV, yet may not be considered "commercial" because of lower service life than expected by the trucking industry.

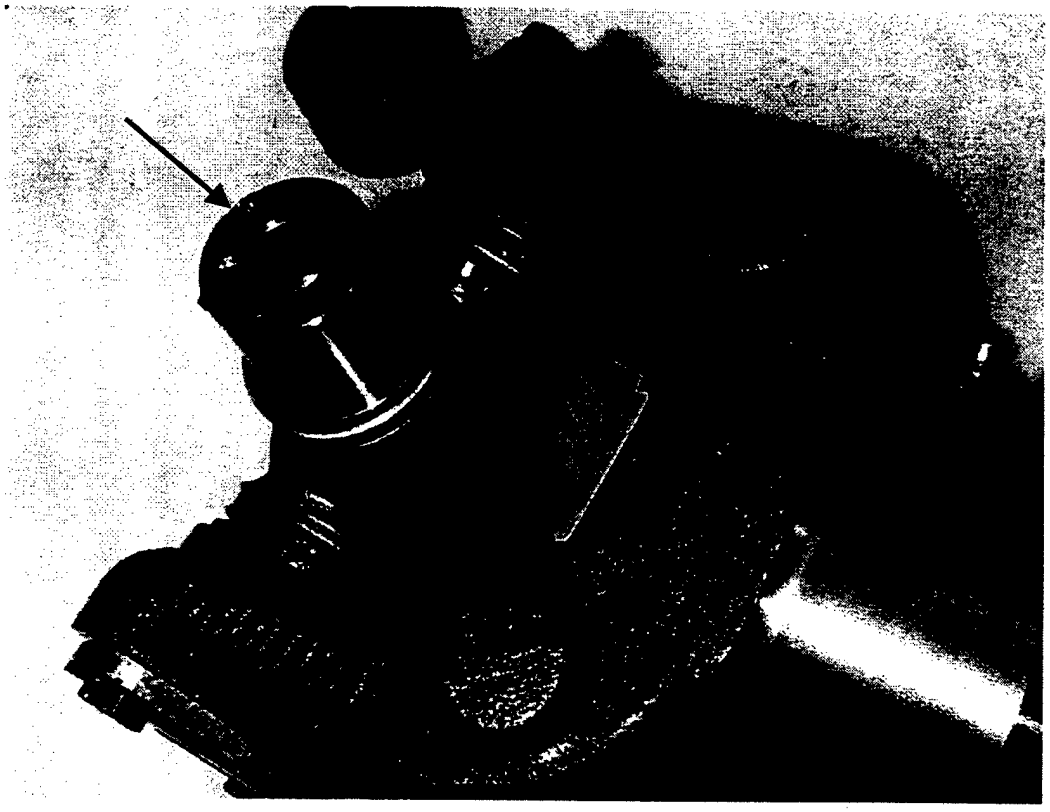

Figure 2.8 Welding of thrust washer to cross of front U-joint of rear driveshaft

3. RECOMMENDATIONS

1) The driveshaft critical speed of approximately 66 Hz needs to be addressed. The SAE recommendation for medium trucks is to have the critical speed 33 percent above the maximum attainable driveshaft speed. If the maximum speed of the vehicle is taken to be 58 mph, then critical speed should be at least 75 Hz. ***This vehicle will likely encounter loads, grades, and wind conditions that will result in speeds higher than 58 mph unless the driver applies service brakes.*** A critical speed frequency of ***at least 85 Hz*** should be required. It should be remembered that the critical speed effect on radial force is not only large at critical speed but begins to amplify forces well below critical speed.

2) The powerpack vertical bending resonance of 43 to 48 Hz can be raised above the vehicle speed range by the substitution of a nodular iron flywheel housing such as the MSC revised design housing. The original Caterpillar housing was of gray cast iron and weighed 54 lbs. Substitution of high strength nodular iron in the original Caterpillar design would raise the resonant frequency about 25 percent, or to about 58 Hz. Since this was deemed an insufficient increase, MSC obtained modified castings of high strength nodular iron and increased the section geometry. The MSC revised design housing weighed 85 lbs. After seeing the results of tests with this MSC design, Caterpillar upgraded their design (CAT 2 version) and obtained similar results. Both the MSC nodular iron flywheel housing and the Caterpillar modified version (CAT 2) approximately double the vertical bending resonant frequency. Since both the stiffened flywheel housings exhibit lateral powerpack bending resonance in the vicinity of 65 Hz, it is imperative that a driveshaft having a critical speed well above 65 Hz be adopted in order to separate the two resonant modes.

3) If only one corrective action is selected, then using the driveshaft having the highest critical speed and tightest balance and run-out tolerances should be the chosen action.

4) The truck could be equipped with an alarm system that would be actuated by excessive vibration at driveline frequency. A sensor could be added to the transfer case, for example, and either alert the operator through the existing readout screen interface, or a stand-alone warning light to signify "maintenance recommended". This appears to be a feasible improvement.

4. OVERVIEW OF PROJECT

4.1 Description of the Failures

A flywheel housing crack typically initiates on the surface of a stiffening web and progresses across the lower portion of the housing decreasing its bending strength and stiffness (see figure 4.1).

Figure 4.1 Typical flywheel housing crack (photograph courtesy of Aberdeen Proving Ground)

The most common driveshaft failure occurs at the rear driveshaft of the LMTV. The driveshaft itself may be bent while the universal joint bearings are frequently found to be loose with evidence of overheating (see figure 4.2). The usual scenario is to find the two bearings of the front U-joint of the rear driveshaft that attach to the transfer case yoke in the most damaged condition. A steel strap referred to as an "easy-service" feature or a "half-round" system retains the caps of these bearings. The other two bearings of the same joint are retained in the driveshaft slip-yoke by a "full-round" support system. No cases have been noted where the full-round supported bearings failed and the half-round supported bearings survived. Adequate initial lubrication of the U-joints was questioned in some early failures due to appearances of failed parts; in some cases even showing rust in the drilled hole of the cross. Lubrication was regarded as a separate, but possibly contributing issue.

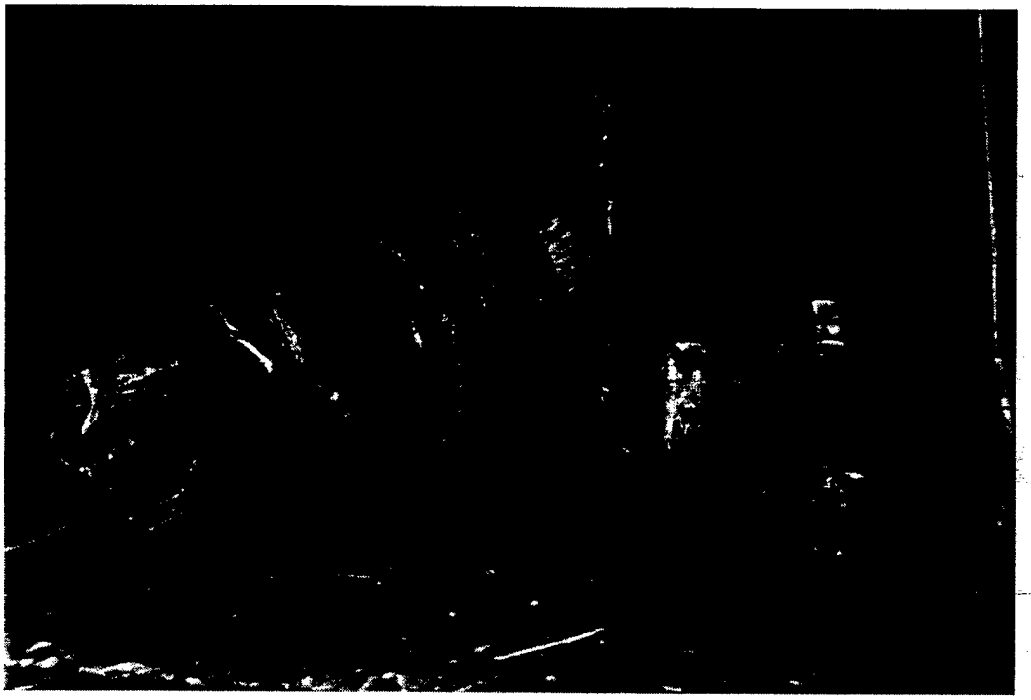

Figure 4.2 Failure of front U-joint of rear driveshaft
(photograph courtesy of Aberdeen Proving Ground)

4.2 Summary of Testing

1) Early information indicated that the vehicle suffered from bending vibration of either the powerpack, the driveshafts, or both. This hypothesis allowed stationary testing of the vehicle in the laboratory. This was accomplished by supporting the vehicle on its tires with the rear axle shafts and front bevel gears removed.

2) Strains were sensed with strain gages applied to the flywheel housing in locations previously selected by Caterpillar. Accelerations were also measured via three-directional accelerometers located at the front and rear of the engine and at the transfer case. Aberdeen Proving Ground investigators selected the locations. Driveshaft speed and engine speed were sensed by magnetic pickups. (Experimental off-road measurements were also made using an instrumented driveshaft, this is discussed in detail in section 6.)

3) Data runs were typically made in seventh gear from a driveshaft speed equivalent to 30-mph ground speed to a maximum attainable driveshaft speed equivalent to 58-mph ground speed. (First order rotational driveshaft frequency is approximately 0.97 times the mph ground speed.) On some runs the need to attain higher speeds above the governed speed was achieved by grounding the front driveshaft. This increased the rear driveshaft speed by virtue of the planetary differential in the transfer case.

4) The operating bending mode shape of the powerpack (see figure 4.3) was obtained by holding the output speed constant at the speed of maximum response and probing the vertical motion of the powerpack with a vibrometer at increments along the length of the powerpack. The plot in figure 4.3 represents the in-phase component of the results. This test was performed with the original production flywheel housing installed. The same test was repeated with a Michigan Scientific nodular iron flywheel housing and did not produce comparable results because the 43 to 48 Hz vertical bending resonant peak was no longer attainable, being replaced by a predominantly lateral bending mode at about 65 Hz.

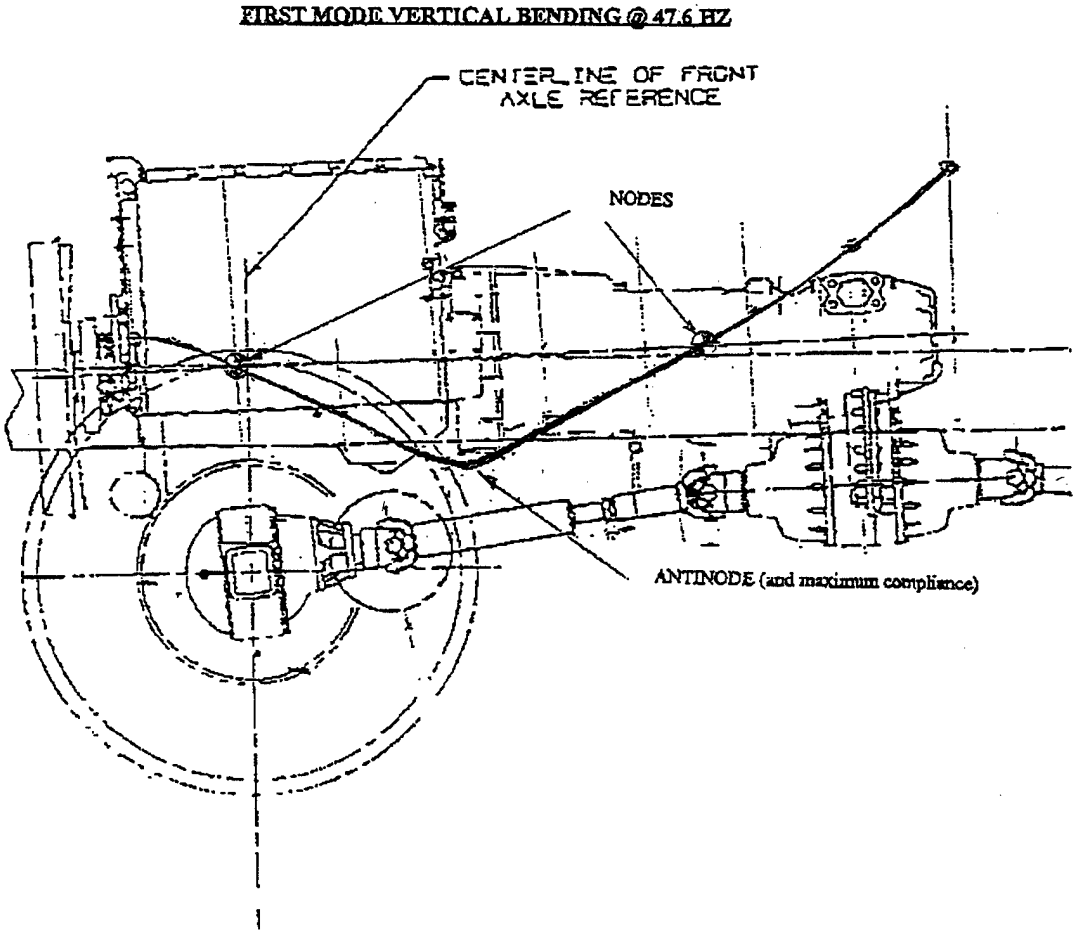

Figure 4.3 Bending mode shape of powerpack

5) The government provided a second truck (Truck #2) for full-scale on-road testing at the General Motors Proving Ground (GMPG) in Milford, Michigan. Instrumentation was essentially identical as noted in item (2) above. A Michigan Scientific revised design nodular iron flywheel housing strain gaged as on the first truck (Truck #1) was installed. GM Allison Transmission Division provided services at GMPG. Data were digitally recorded primarily on the 4-mile circular track at the maximum speed attainable with a slow-down once per lap to 40-mph in order to essentially duplicate the testing being done at Aberdeen Proving Ground on other vehicles. Samples of the data are contained in Volumes 1, 2, 3, & 4 of the *Experimental Data Appendix to Master Report.*

6) The results of bending stiffness measurements comparing the original flywheel housing to the MSC revised design nodular iron flywheel housing are shown in figure 4.4. The measurements were made by suspending a rigid steel bar from the powerpack and using a dial indicator to measure deflections as a vertical force was applied to the powerpack at the flywheel housing. Similar methods were used in the lateral direction to obtain data for use in the computer model of the powertrain.

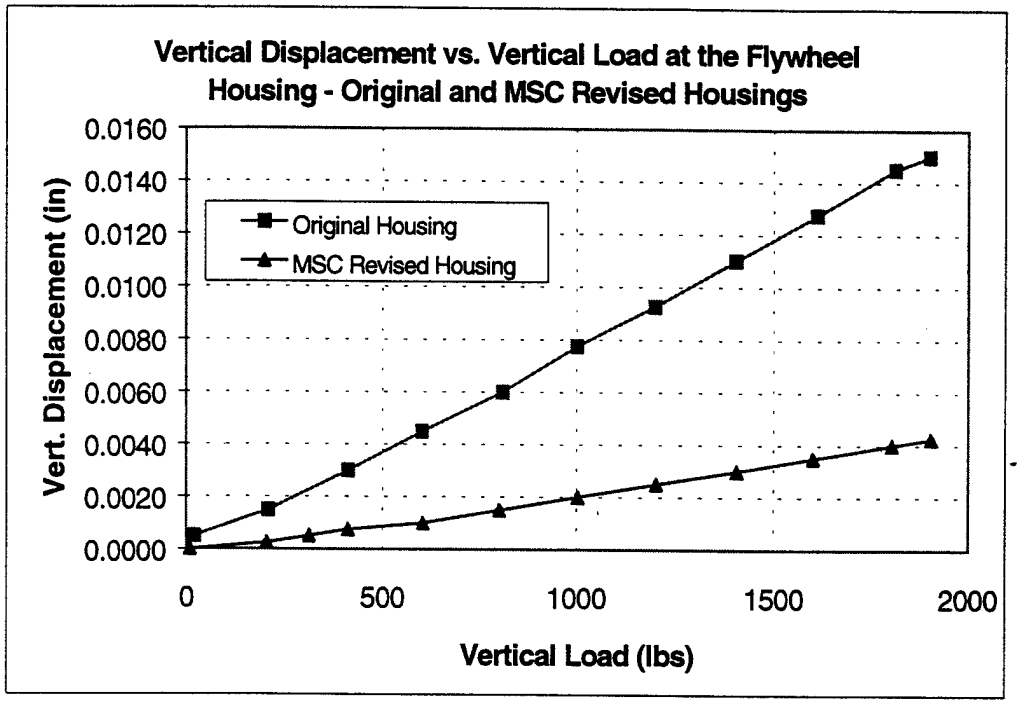

Figure 4.4 Comparison of flywheel housing stiffnesses, original vs MSC versions

4.3 Driveshaft Design Features

The slip-spline engagement length to diameter ratio of 1.55 of the production driveshaft is below the minimum of 2.0 recommended by SAE for commercial use. This undesirable feature is compounded by nylon coating the spline surface to obtain a lower coefficient of friction. The 0.010 inch thickness of nylon coating adds elasticity to the joint and also deforms in service such that the looseness (referred to as hinging) allows the mass of the driveshaft to orbit at some distance from its intended center of rotation. This characteristic plus the static unbalance and bending of the driveshaft due to the centrifugal loading results in radial force magnitude as high as 1000 lbs. This order of magnitude is confirmed by measurements made with the instrumented driveshaft as discussed in section 6.

One of the parameters that determine the driveshaft's critical speed is lateral stiffness or compliance. The major compliance of the driveshaft is due to the splined section of the slip-yoke. This was shown by the computer model developed by MSC and was evident in Meritor's ADAMS model (see section 5.7.1). This was also shown by reversing the driveshaft end-for-end which consistently lowered the excitation to the transfer case. Also, driveshafts that were run above critical speed at MSC were found to be yielded in the spline section rather than the tube section. The necked-down spline section should be as large in diameter as practical. The engagement should be 5 inches or more if a 2½ inch diameter spline is chosen in order to meet the minimum SAE (and Meritor) recommendation of a 2.0 length/diameter ratio. The design of the driveshaft should maximize the ratio of the section modulus to the mass-per-unit-length. Details of an improved driveshaft are found in section 5 of this report.

MSC was directed to fabricate a "proof of principle" driveshaft that would minimize hinging. A sleeve tube was welded over the spline section and provided a close fit over the outside diameter of the yoke. The results in terms of flywheel housing strains were comparable to having no driveshaft installed. The computer model indicated that the critical speed frequency of the "proof of principle" driveshaft is about 85 Hz.

5. COMPUTER MODEL OF LMTV DRIVELINE

5.1 Model Description

A computer model of the LMTV driveline was developed to assist in studying resonant behavior of drivetrain components and to better understand the complex dynamics of the drivetrain and facilitate parameter studies.

The model was created using Dynamic Analysis and Design System* (DADS) software. DADS is a computer simulation tool that is used to predict the behavior of single or multi-body mechanical systems. DADS allows the user to graphically construct models of mechanical systems. DADS can output the positions, velocities, accelerations, and reaction forces of all bodies modeled.

5.2 Model Construction

Driveline model construction began by first creating eleven bodies that are representative of the driveline. The bodies are shown in figure 5.1.

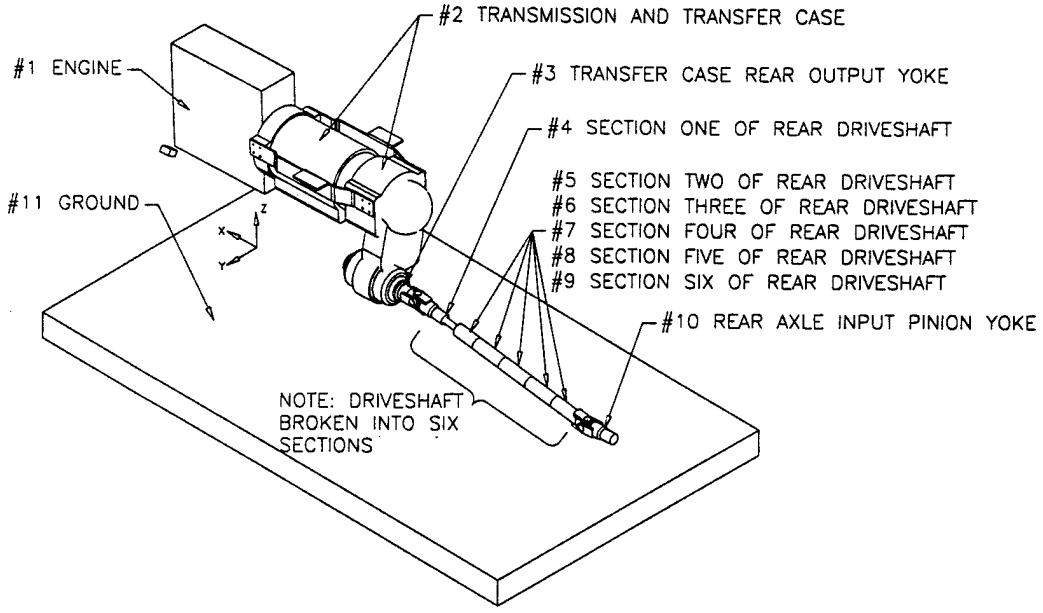

Figure 5.1 MSC DADS model configuration

* Trademark of Computer Aided Design Software Inc., Coralville, Iowa.

The following bodies were included in the model:

1. Engine
2. Transmission and Transfer Case
3. Transfer Case Rear Output Yoke
4. Section One of Rear Driveshaft
5. Section Two of Rear Driveshaft
6. Section Three of Rear Driveshaft
7. Section Four of Rear Driveshaft
8. Section Five of Rear Driveshaft
9. Section Six of Rear Driveshaft
10. Rear Axle Input Pinion Yoke
11. Ground

Note the transmission and transfer case were modeled as one rigid body and that the driveshaft was broken into six bodies in order to separately model the hinging effect of the slip spline and the driveshaft bending stiffness. The model connects the bodies listed above with springs and/or joints.

The engine and transmission/transfer case were connected to ground through bi-directional springs (springs that have compressive and tensile spring rates). Each engine and transmission mount was modeled by three bi-directional springs; therefore, a total of twelve bi-directional springs were used to connect the engine and transmission/transfer case package to ground at the four mount locations.

The six driveshaft bodies were connected together by five bushing elements. Bushing elements in DADS are spring-like elements that allow six degrees of freedom (three translations and three rotations). One additional bushing representing elasticity of the flywheel housing was used to connect the engine to the transmission.

The ends of the driveshaft were joined to the transfer case and rear axle input pinion yokes by universal joints. The two U-joints were correctly phased with one another. Creating a simple model in DADS that included one U-joint model element running at an angle checked the validity of the DADS supplied U-joint modeling element. While driving the U-joint input at a constant angular speed, the output angular speed was compared to analytical results and found to be valid.

Two revolute joint elements were placed in the model. A revolute joint element in DADS is a joint that allows only one rotational degree of freedom. One revolute joint was used between the transmission/transfer case assembly and the transfer case rear output yoke. The other revolute joint was used between the rear axle input pinion yoke and ground. Prescribed rotation of the driveshaft was achieved by either a control system that applied a torque to the transfer case rear output yoke or a driver that defined the angular position as a function of time.

5.3 Spring Rates, Inertias, and Damping

Values for the spring rates used in the model were either supplied by the manufacturer, experimentally measured, or analytically calculated. Barry Controls supplied engine and transmission mount rates. Meritor supplied the driveshaft torsional spring rate. The lateral and vertical powerpack bending stiffnesses were experimentally measured (see Appendix A). The stiffness of the slip yoke and necked down portion of the driveshaft was experimentally measured by measuring the static deflection of the driveshaft's front U-joint when cantilevered from a rigid support (see Appendix B). Bending, axial, and radial spring rates for each of the driveshaft tubes modeled were analytically calculated based on the cross section, length, and material type. See figure 5.2 for all of the spring locations used in the model (the stiffness values shown in the figure are those for a configuration with an MSC flywheel housing and Meritor original production driveshaft).

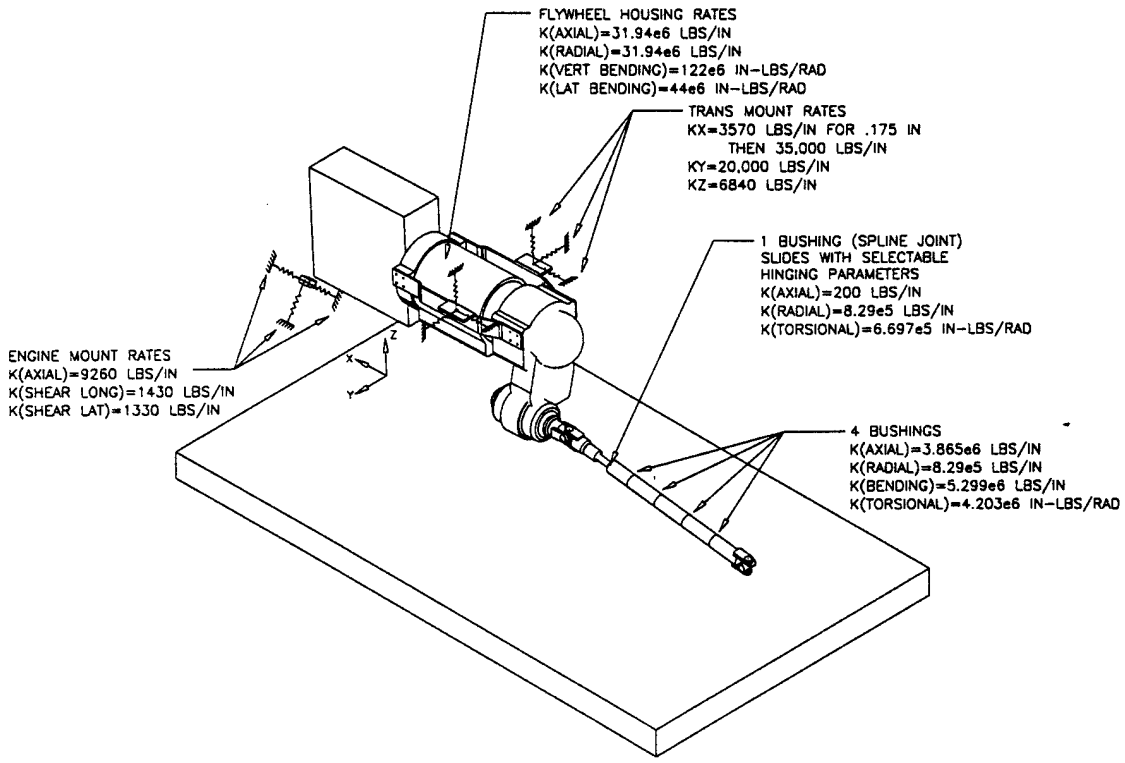

Figure 5.2 MSC DADS model configuration showing stiffness locations
(stiffness values shown are for a configuration with an MSC flywheel housing and a Meritor original production driveshaft)

Caterpillar and Allison Transmission supplied inertia values for the engine and transmission/transfer case assembly respectively. Adjustments to the engine inertia were made to include the effect of the generator. DADS automatically calculated inertias of standard shapes such as tubes and cylinders. Unknown inertias such as the ring and pinion of the rear axle were estimated, remembering to include gear ratios. The inertias used in the model are shown in figure 5.3 (the inertia values shown in the figure are those for a configuration with an MSC flywheel housing and Meritor original production driveshaft).

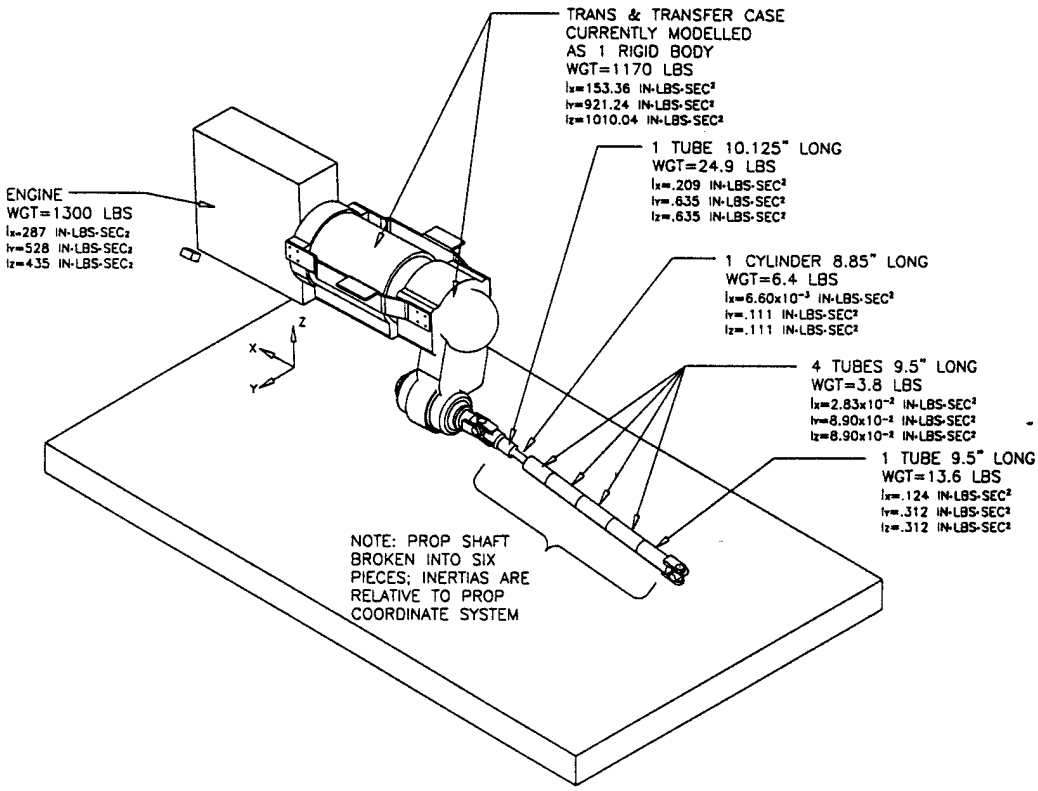

Figure 5.3 MSC DADS model configuration showing inertia locations
(inertia values shown are for a configuration with an MSC flywheel housing and a Meritor original production driveshaft)

Damping was determined by using experimental data or estimating the values based on conventional modeling practice.

5.4 Limitations of the Model

The model is a dynamic model that outputs magnitude and frequency response of the following:

1. Linear and angular displacements
2. Linear and angular velocities
3. Linear and angular accelerations
4. Reaction forces and moments

The model does not give stresses or strains; however, the forces and moments could be used as load cases in finite element models to estimate resulting stresses and strains. The model will not output or predict temperatures of U-joints or slip splines, spline wear or fatigue life of the components.

5.5 Assumptions

At the time the model was constructed it was assumed that drivetrain torsional response was not of significant importance; therefore, the internal components of the engine, transmission, transfer case, and rear axle were not included in the model. The rear axle was not modeled; only the rear pinion input yoke was included. It was assumed, based on experimental findings, that the front driveshaft was of significantly less concern than the rear driveshaft because of its much smaller length.

5.6 Model Validation

Performing experimental measurements on the vehicle aided validation of the model. One measurement consisted of shining a strobe light on the driveshaft while it rotated and measuring driveshaft deflection. Early model results indicated similar driveshaft deflection magnitudes. Comparing experimentally measured flywheel housing frequency response with the model output of powerpack bending angle frequency response provided additional information for validation of the model.

An instrumented driveshaft was used for further model validation. This driveshaft measured front U-joint forces, driveshaft bending moment, driveshaft thrust, and driveshaft torque. These experimentally measured quantities were compared to the corresponding computer model outputs. Adjustments to the computer model were made until a clear correlation within reasonable limits of measurement precision resulted.

5.7 Driveshafts Modeled

The following driveshafts were modeled:

1. Meritor Original Production Driveshaft
2. MSC Proof of Principle Driveshaft (Sleeved)
3. Proposed Driveshafts
   a) Meritor Interim Design
   b) Meritor A1 Design
   c) MSC Revised Design
4. Instrumented Meritor Original Production Driveshaft (Used for Model Validation)

5.7.1 Meritor Original Production Driveshaft

The first driveshaft modeled was the Meritor original production driveshaft. This driveshaft had a 3.50" O.D. X 0.134" wall tube and a 2.00" O.D. X 3.1" long polyglide coated splined shaft with 16 splines. Meritor had created an ADAMS model of this driveshaft and determined the first mode bending frequency to be 72.8 Hz. The Meritor ADAMS model first mode bending simulation of this driveshaft is shown in figure 5.4.

MERITOR ORIGINAL PRODUCTION DRIVESHAFT 1st MODE BENDING
(SIMPLY SUPPORTED)
MERITOR ADAMS MODEL
Frequency=72.8 Hz

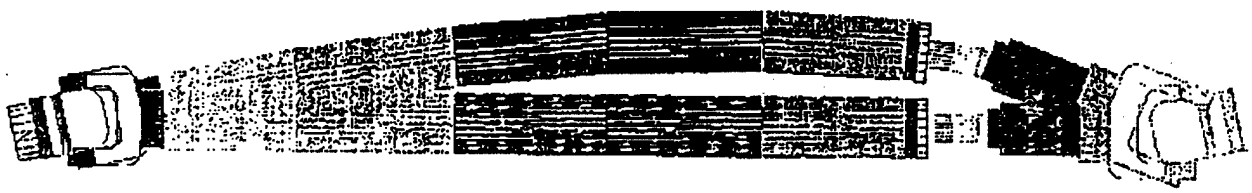

Figure 5.4 Meritor ADAMS model of original production driveshaft

The mode shape of the ADAMS model is comparable to the results obtained with the MSC DADS model; however, the MSC DADS model predicted a critical speed of 66 to 67 Hz. This is lower than the 72.8 Hz predicted by the ADAMS model. Factors that could effect the results of the ADAMS model computed frequency are listed below:

1. The ADAMS model was created with beam elements: compliance of the spline area was not included.
2. It was assumed that the installed length of the driveshaft was 59", it is actually 61.875" long.
3. The MSC DADS model includes the effects of the transfer case reactance, the ADAMS does not.

In the MSC DADS model the Meritor original production driveshaft was modeled by dividing the driveshaft into six bodies. These six bodies were connected by a total of five bushing elements and the appropriate stiffness entered for each bushing. The complete driveshaft assembly was then connected by universal joints to the transfer case rear output yoke and the rear axle input pinion yoke. As noted above, the model results indicated a 1st mode bending frequency of 66 to 67 Hz, see figure 5.5.

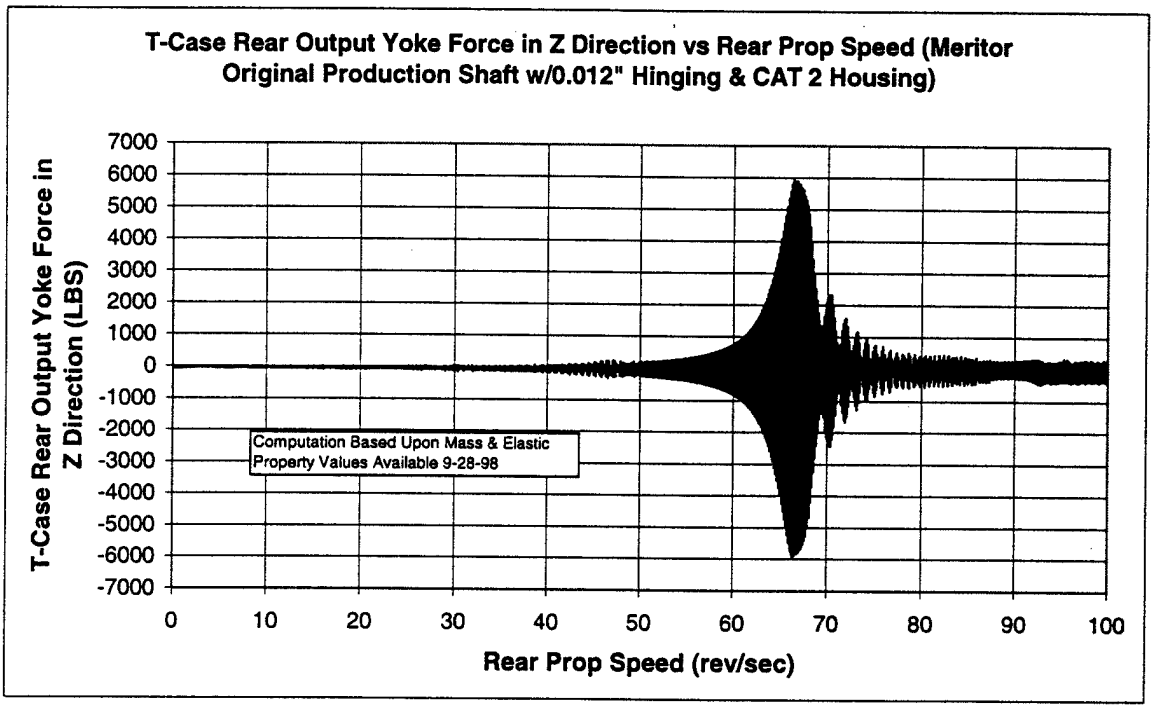

Figure 5.5 MSC DADS model output of Meritor original production driveshaft

The MSC DADS computer model animations of the Meritor original production driveshaft showed that as resonance is approached, the driveshaft deflects like a jump rope. The "heavy side" of the driveshaft deflects outward and orbits around the center of rotation of the driveshaft.

The deflection of the driveshaft induces large centrifugal loads on the U-joints. The front U-joint forces are transmitted to the transfer case and act as an exciter to the powerpack bending vibration.

5.7.2 MSC Proof of Principle Driveshaft

The Meritor original production driveshaft with a 2.00" O.D. splined shaft and a long 1.633" O.D. necked down portion was recognized as having a low relative bending stiffness; therefore, a tight fitting reinforcing tube was added to bridge this area of the driveshaft, see figure 5.6.

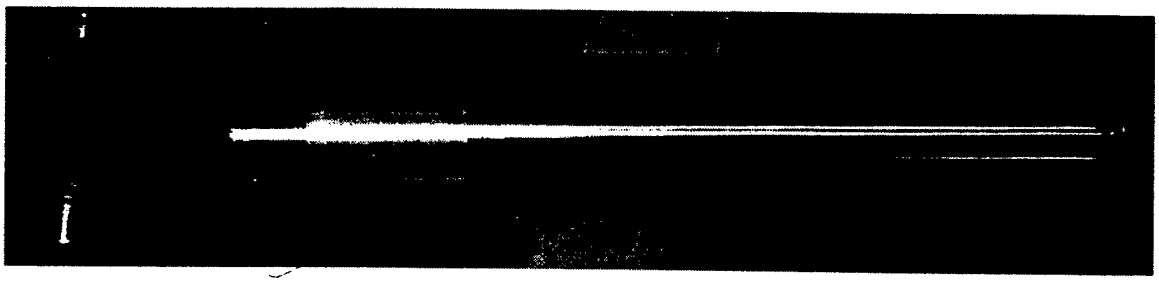

Figure 5.6 Photograph MSC proof of principle driveshaft

The driveshaft in figure 5.6 was called the MSC proof of principle driveshaft, and was also modeled.

Experimental measurements made with the MSC proof of principle driveshaft installed in a vehicle indicated a significant reduction of flywheel housing strains when compared to the Meritor original production driveshaft. The experimental results indicated the benefit of stiffening the "hinge" area. Model results for the MSC proof of principle driveshaft model are shown in figure 5.7.

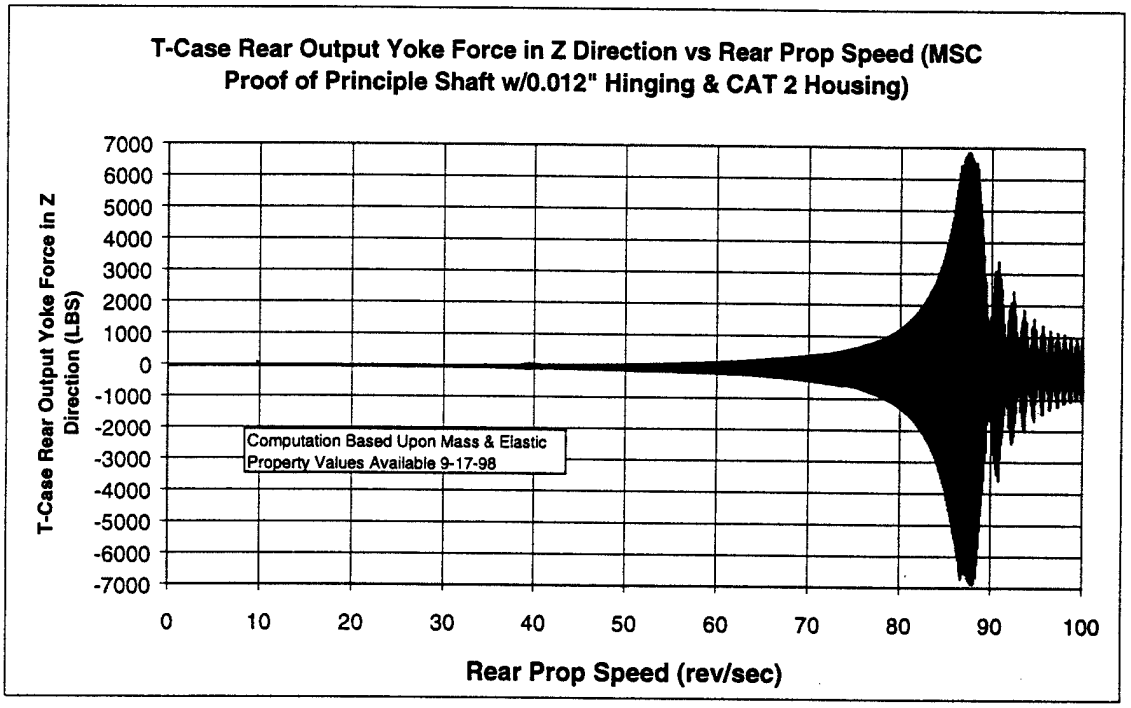

Figure 5.7 MSC DADS model output of MSC proof of principle driveshaft

Note that the resonant frequency is shown to have increased to 87-88 Hz. Clearly, it was found that increasing the spline bending stiffness would be extremely beneficial.

5.7.3 Proposed Driveshafts

Three proposed driveshafts were modeled: i) Meritor interim: similar to the original but with a 4" O.D. tube and 3.23" long spline, ii) Meritor A1: similar to the original but with a 4" O.D. tube and 3.85" long spline, and iii) MSC revised design. The interim driveshaft was first modeled using a spline hinge stiffness value the same as that measured for the Meritor original production driveshaft. Figure 5.8 shows the results of this model.

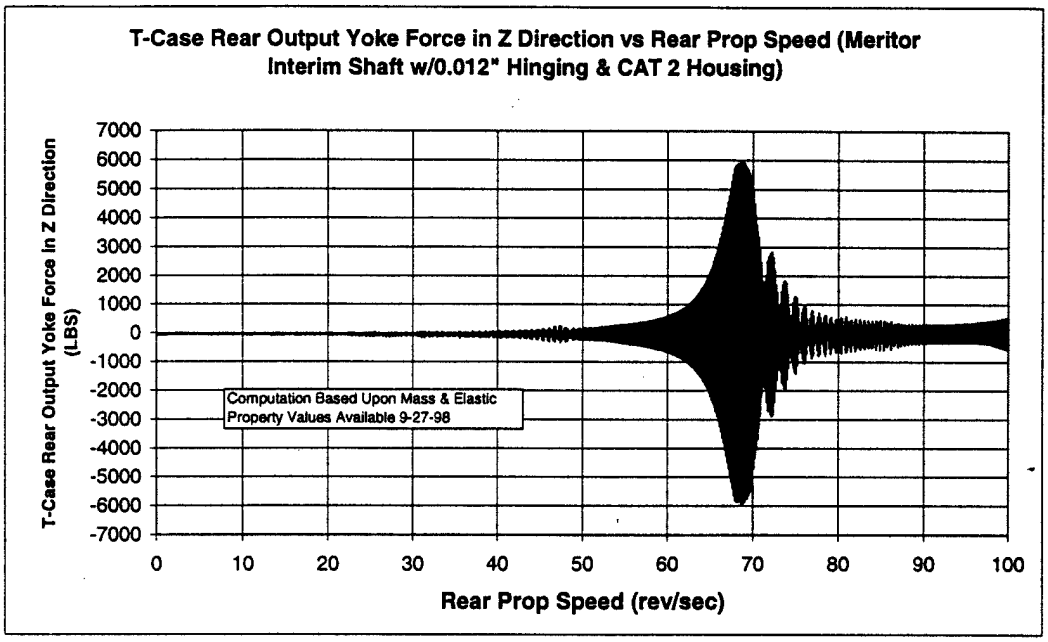

Figure 5.8 MSC DADS model output of Meritor interim driveshaft: similar to original but with a 4" O.D. tube and 3.23" long spline (original production driveshaft hinge stiffness used in model)

Note the model output of the interim driveshaft indicated a resonant frequency of 68-69 Hz. The model output for the Meritor A1 driveshaft is shown in figure 5.9.

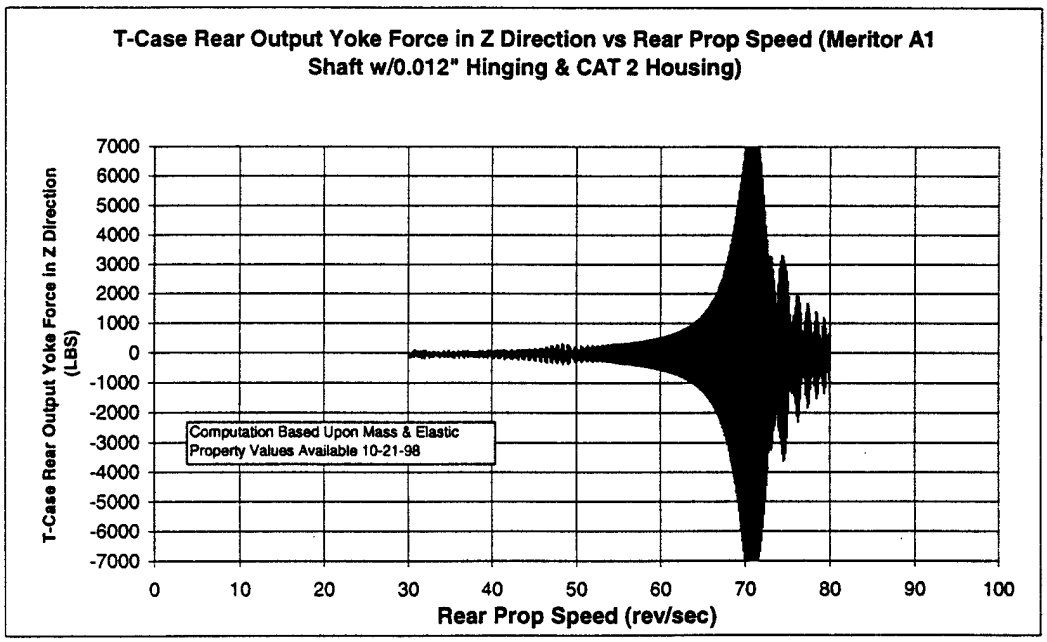

Figure 5.9 MSC DADS model output of Meritor A1 driveshaft: similar to original but with a 4" O.D. tube and 3.85" long spline (A1 measured hinge stiffness used in model)

The A1 driveshaft model indicated a resonant frequency of 70-71 Hz. The measured hinge stiffness for the A1 driveshaft spline section was higher than that measured for the Meritor original production driveshaft. The slight increase in hinge stiffness of the A1 driveshaft was due to the increased engagement length of the slip spline.

The computed frequency response of the A1 driveshaft model was found to be within 3 percent of the experimentally found frequency resonant response of an A1 driveshaft run through critical as indicated by flywheel housing strains, see figure 5.10.

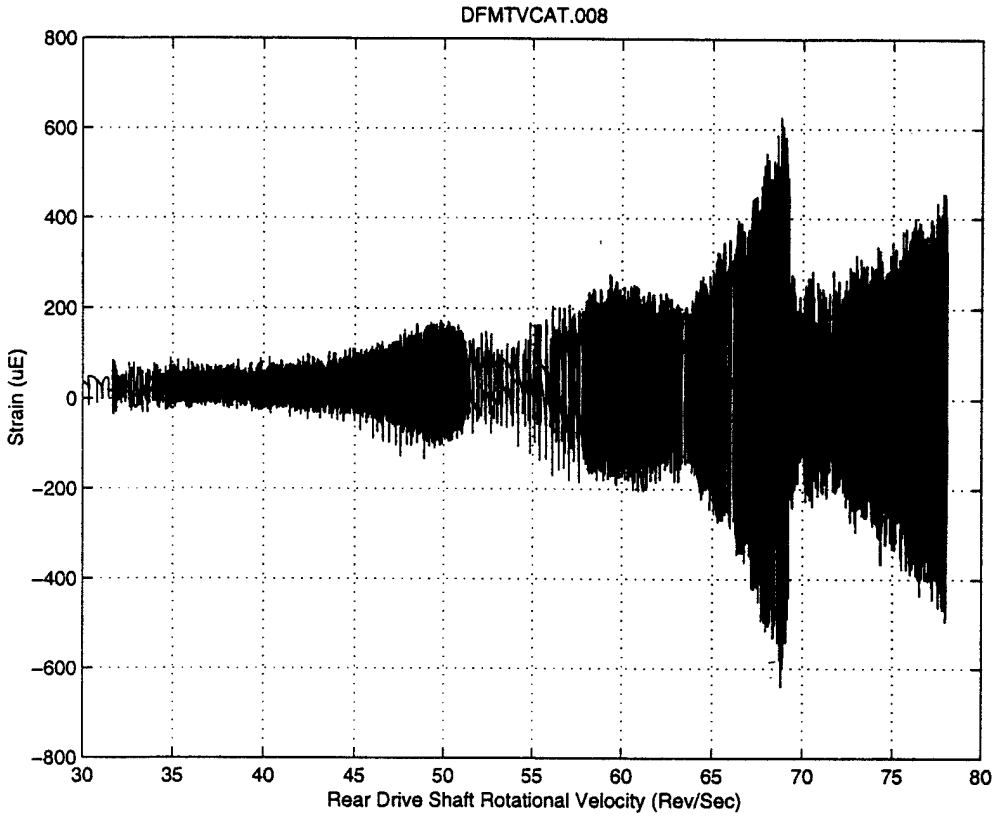

Figure 5.10 CAT 2 flywheel housing typical strain response with Meritor A1 driveshaft, 30 mph to top speed, front driveshaft grounded, no unbalance added, seventh gear

The MSC revised design driveshaft has a less massive 4.00"O.D. X 0.109" wall tube and a 2.5" O.D. spline with 6" of spline engagement. See figure 5.11 for a dimensioned drawing.

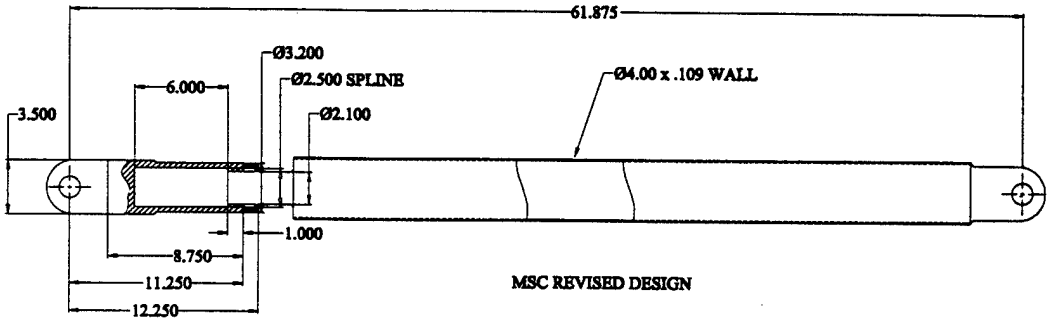

Figure 5.11 MSC revised design driveshaft (dimensions in inches)

The MSC DADS model output of the MSC revised design driveshaft indicated a resonant frequency of 86-87 Hz as shown in figure 5.12.

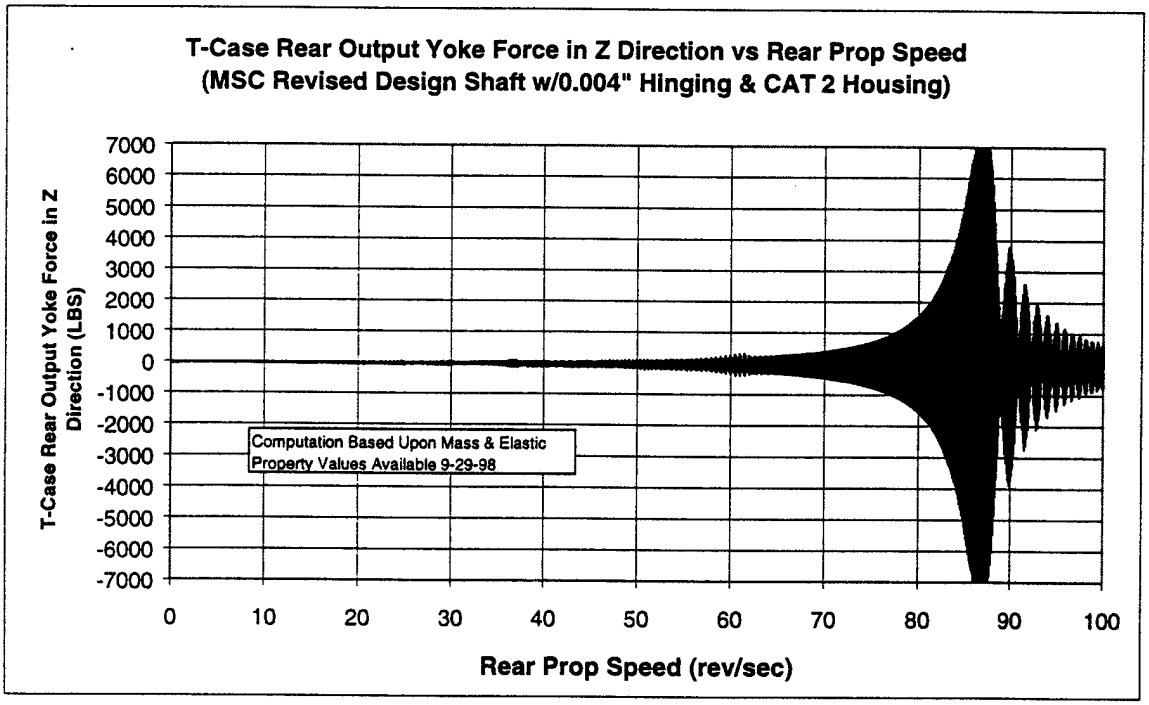

Figure 5.12 MSC DADS model output of MSC revised driveshaft

5.7.4 Instrumented Meritor Original Production Driveshaft

A Meritor original production driveshaft was instrumented to experimentally measure forces, moments and universal joint temperatures. A picture of the driveshaft is shown in figure 5.13. A detailed discussion of this instrumented driveshaft and the data measured with it are contained in Section 6.

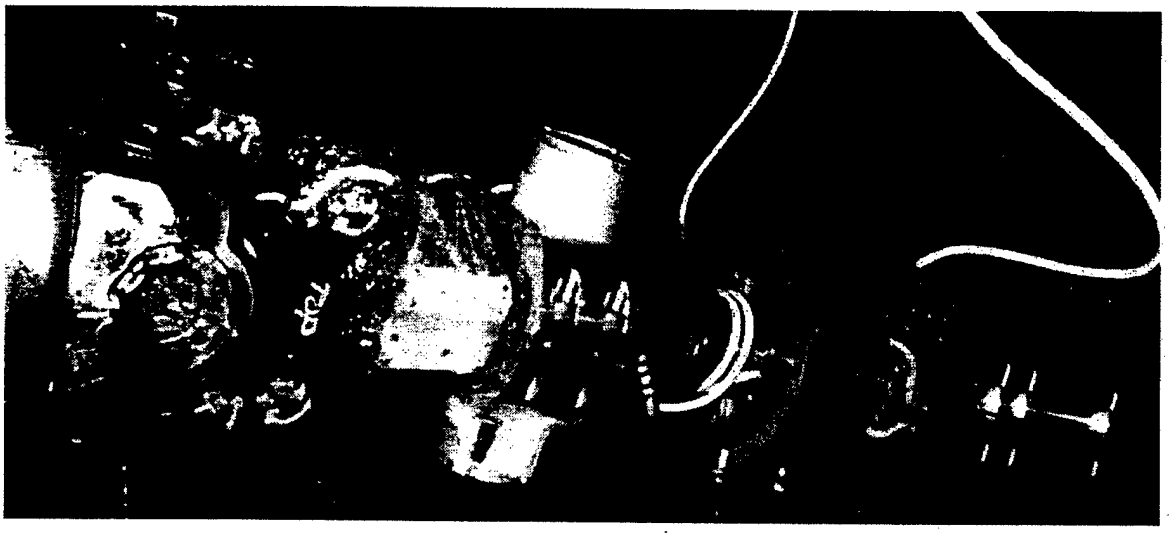

Figure 5.13 Instrumented Meritor original production driveshaft

Modifications were made to the Meritor original production driveshaft computer model that accounted for the added mass and inertia of the instrumentation added to the driveshaft. Pre and post test total indicated run-out (TIR) measurements of the instrumented driveshaft are given in Appendix C. TIR was accounted for in the model by offsetting the center of gravity (cg) of the six sections of the driveshaft to the post test TIR condition. The offsetting produced a net unbalance in the direction of the offset cg's. Inserting a counter balance weight in the model opposite the offset cg's minimized the unbalance. In the process of counterbalancing, wide variations in U-joint force magnitudes were observed with small changes in the magnitude of counterbalance. This observation and previous work with straight driveshafts indicates that driveshafts with high TIR are more problematic to balance than those that are nearly straight.

As discussed earlier, the prior DADS models contained a total of eleven bodies and six bushings. However, the instrumented driveshaft model had two additional bodies and bushings. These elements were included to model 1) the compliance between the transfer case rear output yoke and the transfer case and 2) the compliance of the rear axle input pinion yoke and the ground. See Appendix D for a picture of the transfer case rear output yoke measurement setup and the data collected. The addition of the transfer case output yoke compliance caused a 3 Hz drop in driveshaft resonant frequency. With the above changes made to the Meritor original production driveshaft model and the driveshaft speed controlled with a control system, the experimental test results of the instrumented driveshaft were compared with the model generated output.

One of the parameters experimentally measured was transfer case rear output yoke U-joint radial (y-z) force. In order to compare model data with experimental data it is most appropriate to use the *vector sum magnitudes* of the components of the *U-joint radial forces*. This is because the stiffness and mass distributions with respect to the model x-y-z coordinate system may not coincide with that of the experimental x-y-z coordinate system. The use of vector sum magnitude of the U-joint radial forces however removes this arbitrariness yet allows a valid comparison with regards to both amplitude and frequency content.

Figure 5.14 shows a comparison of model results and experimental data. The test run consisted of a ramp up and then decrease of driveshaft speed as shown. Both plots show eighteen seconds of data.

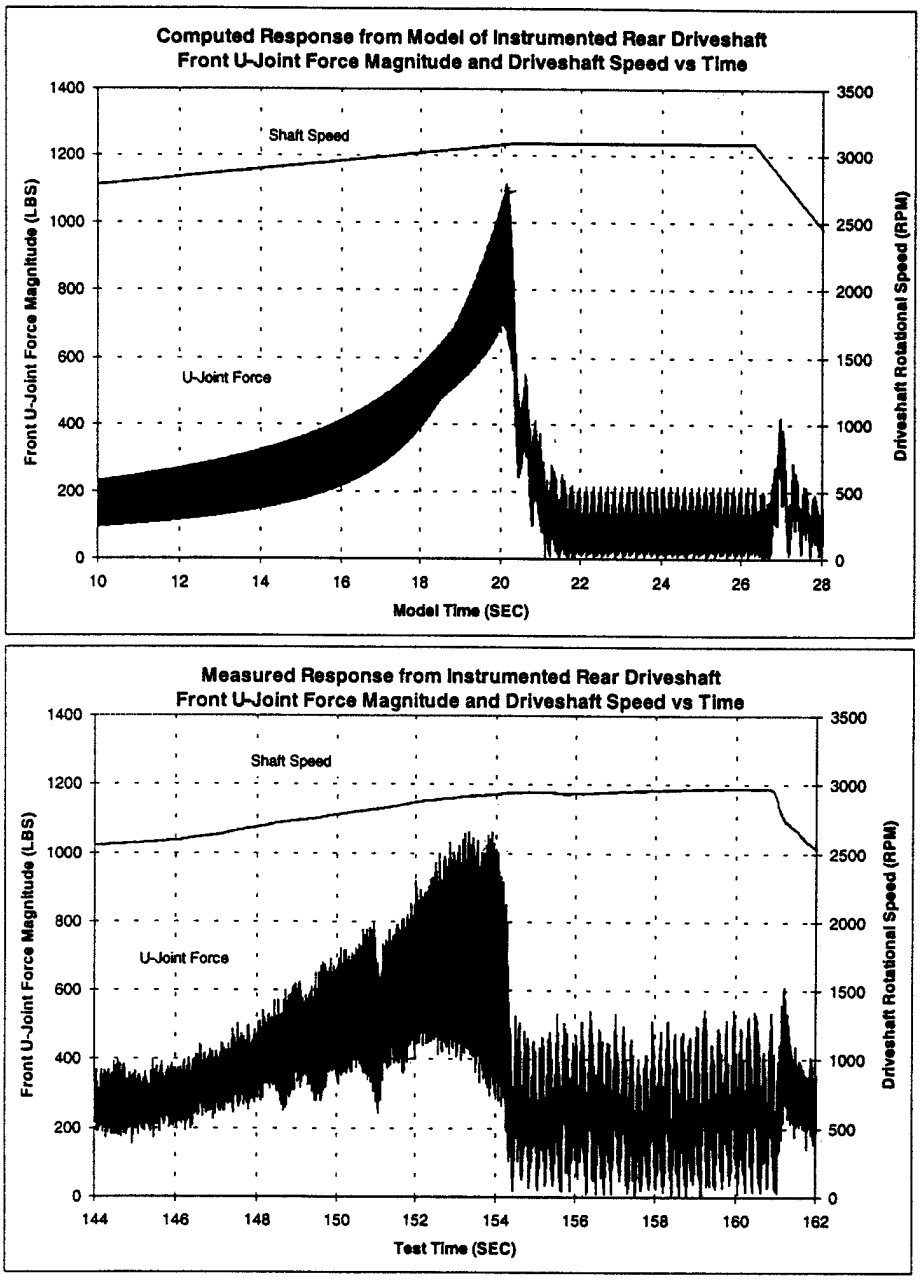

Figure 5.14 Model output vs experimental data for front U-joint force of rear driveshaft

The model results appear to reasonably agree with the experimental data. Note the equivalent maximum force magnitudes of approximately 1000 pounds. These occur at a driveshaft speed of 2900 RPM to 3100 RPM or 48 Hz to 52 Hz, i.e. the critical speed. It is important to understand that the critical speed of the instrumented driveshaft is lowered by the added mass of the instrumentation. As noted above, this mass was also added to the computer model for correlation of computed and measured dynamic responses. Figure 5.15 show the same data in figure 5.14 but with a rescaled time axis so frequency content can be examined more clearly.

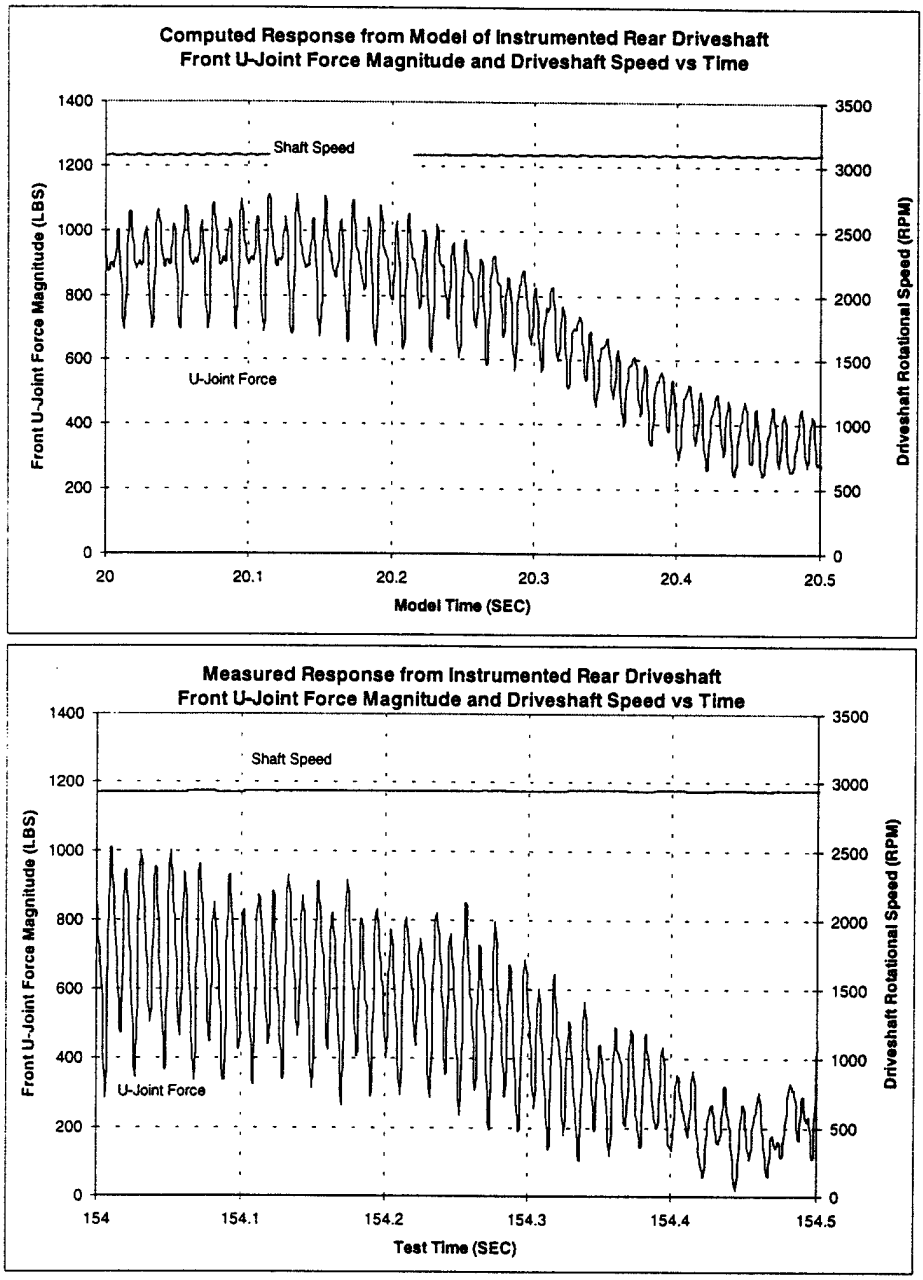

Figure 5.15 Data of figure 5.14 with rescaled time axis

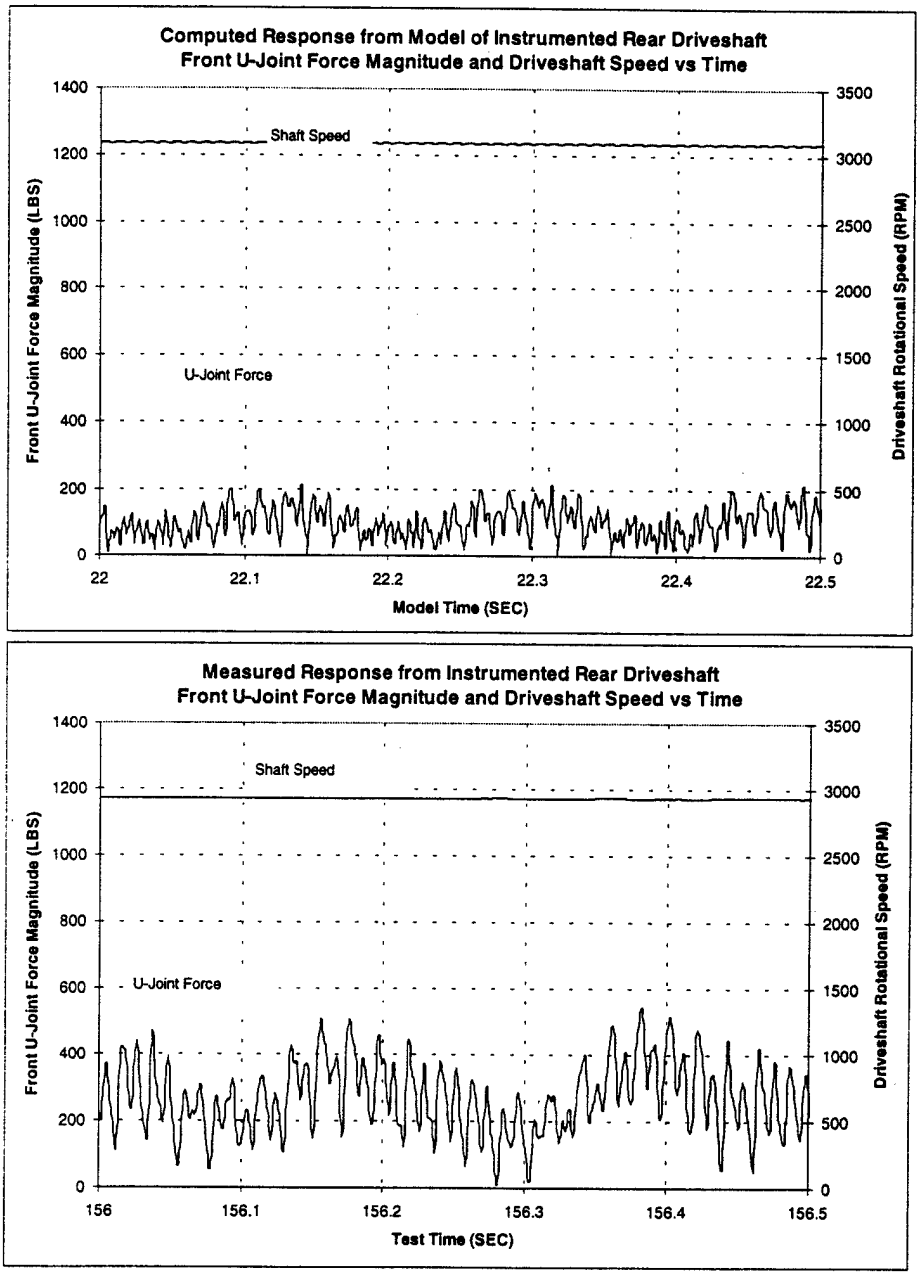

Figure 5.15 (continued) Data of figure 5.14 with rescaled time axis

Figure 5.16 shows the model results of U-joint radial z direction force for the instrumented driveshaft. This plot is in the same format as model results of the other driveshafts previously discussed and therefore is useful for comparison.

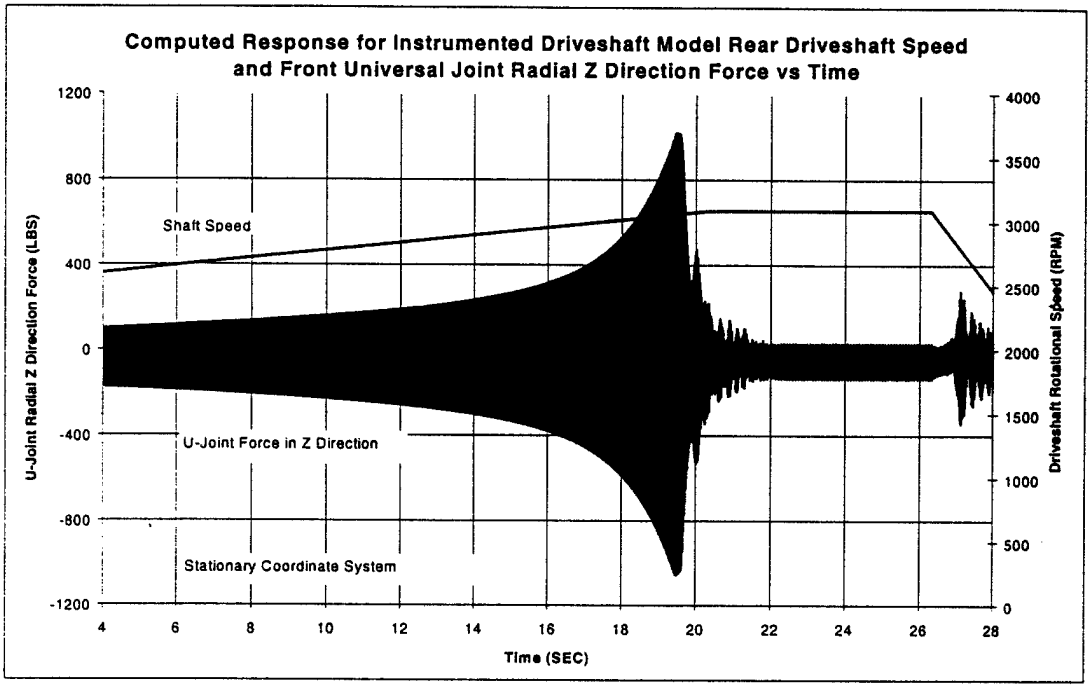

Figure 5.16 MSC DADS model output of U-joint force in Z direction, instrumented Meritor original production driveshaft

Generally, all driveshafts appear to have been modeled correctly; however, the instrumented driveshaft model brought to light the importance of including transfer case rear output yoke compliance and driveshaft damping magnitudes. Model results show that small changes in damping, unbalance, or shaft straightness cause enormous changes in the dynamic response of the system near resonance. This is also supported by results obtained via various on road vehicle testing. It clearly illustrates the folly of operating near the shaft critical speed. It is essential to raise the shaft critical speed as high as possible.

6. EXPERIMENTAL MEASUREMENTS OF REAR DRIVESHAFT DYNAMICS

6.1 Introduction

In support of fulfilling the contract requirement, experimental measurements of the vehicle's rear driveshaft dynamics were performed. Also in support was the development of a computer model that simulated major components of the powertrain including the rear driveshaft (see section 5 for a discussion of the computer model). The experimental measurements, in addition to providing insight into the dynamic behavior of the rear driveshaft, were used to validate the computer model. Once validated, the model was used to better understand the system dynamics and to provide recommendations for corrective actions. This section discusses the methodology of the rear driveshaft experimental measurements conducted and presents a summary and analysis of the experimental data.

The test vehicle supplied to MSC was an M1078 series, 2½ ton, 4X4 LMTV, serial number AT0357B-AC equipped with a 225 hp 6 cylinder in-line turbo-charged diesel engine (Caterpillar model 3116 ATAAC), 7 speed automatic transmission (Allison MD3070PT), a Caterpillar MOD II flywheel housing, and an overall rear axle ratio of 7.8. Illustrations of the test vehicle are shown in Figure 6.1.

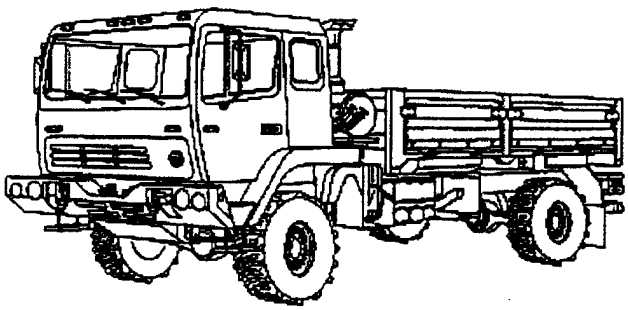

LEFT FRONT VIEW

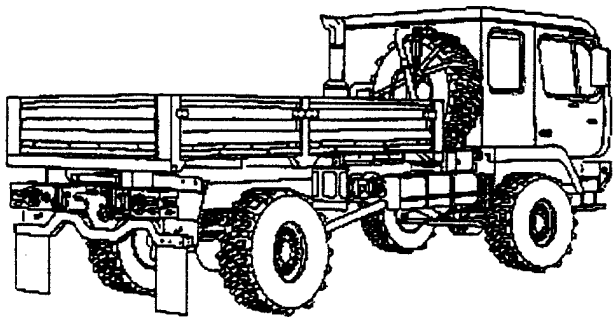

RIGHT REAR VIEW

Figure 6.1 Illustrations of M1078 2½ ton, 4X4, dropside, LMTV cargo truck (Figure 1.1 repeated)

6.2 Results

1) A speed sweep of the instrumented rear driveshaft resulted in a sharp rise of forward U-joint radial force as sensed at the U-joint cross. The sharp rise occurs at approximately 2930 RPM (49 Hz 1st order) and corresponds to an approximate road speed of 50 mph. This force (with respect to stationary vehicle coordinates) is primarily composed of 1st order driveshaft rotational frequency and has a peak load magnitude of approximately 1000 pounds. A sharp rise of driveshaft bending moment as sensed six inches aft of the splined shaft weld joint was also observed at 2930 RPM. This bending moment (with respect to stationary vehicle coordinates) is also primarily composed of 1st order driveshaft rotational frequency and has a peak magnitude of approximately 560 lbft.

2) Once the instrumented driveshaft speed gets above 2930 RPM, both U-joint radial force and driveshaft bending moment magnitudes (with respect to stationary vehicle coordinates) decrease and develop a 5 Hz beat. The peak magnitudes decrease to approximately 40% to 50% of the values stated in result (1).

3) The driveshaft thrust force increases as driveshaft speed approaches 2930 RPM. The force at this speed is primarily 1st order driveshaft rotational frequency and is entirely compressive with a peak-to-peak value of about 70 to 540 pounds.

4) No yielding of the driveshaft occurred at the locations of the strain gages; however, the driveshaft did yield elsewhere as indicated by the pre- and post-test run-out measurements given in Appendix C.

6.3 Measurement Methodology

The following parameters were measured:

1. REAR DRIVESHAFT TORQUE (Mx)
2. REAR DRIVESHAFT FORE/AFT THRUST (Fx)
3. REAR DRIVESHAFT BENDING, TWO ORTHOGONAL PLANES (My & Mz)
4. FORCES AT THE FORWARD U-JOINT OF THE REAR DRIVESHAFT, TWO DIRECTIONS (Fy & Fz)
5. REAR DRIVESHAFT SPEED

Configuration of the rear driveshaft instrumentation assembly included provisions to measure temperatures at each of the four bearing caps of the forward U-joint. Although these measurements were not needed as part of the investigation of driveshaft dynamics per se and are beyond the scope of this report, there was interest in the amount of heat generated at these locations and it was efficient to include provisions for implementing these measurements as part of the instrumentation assembly to study the driveshaft dynamics.

Note that all of the parameters listed above are measured with respect to a rotating coordinate system i.e. a system that rotates with the rear driveshaft. All driveshaft signals were statically zeroed with the driveshaft x,y,z rotating coordinate system (as marked on the driveshaft) aligned with SAE x,y,z vehicle coordinate directions. The signal polarities *in this alignment condition* are as follows:

Positive torque data is SAE *negative* Mx
Positive thrust data is shaft compression
Positive bending about y-axis data is SAE positive My
Positive bending about z-axis data is SAE positive Mz
Positive U-joint force in y direction data is slip yoke pushing in *negative* SAE y direction
Positive U-joint force in z direction data is slip yoke pushing in positive SAE z direction

Driveshaft torque, thrust, and the two orthogonal planes of bending were sensed by mounting full bridge strain gage circuits on the outside diameter of the driveshaft tube approximately six inches aft of the splined shaft weld joint. A thin-walled aluminum shell extended over the gaged area to protect the gages. The shell also served as a housing for locating strain gage bridge amplifiers close to the strain gage bridges. (Locating the amplifiers close to the strain gage bridges helps reduce noise problems, this will be discussed in section 6.4.)

Mounting strain gages sensitive to shear forces on each of the four arms of the forward U-joint cross sensed forces in the y and z directions. The cross was machined to provide symmetry, sensitivity, and acceptable gage mounting surfaces without compromising strength and stiffness. These strain gage bridges also had amplifiers located close-by via mounting them to an aluminum collar that was attached to the outside diameter of the slip yoke. Mounted in tandem with these amplifiers were two thermocouple conditioning amplifier units (2 channels per unit) used to condition thermocouple junctions that were located at the center of the faces of the four U-joint bearing caps.

Two adjacent through-bore slip rings were used to conduct power and control signals to the aforementioned amplifiers and provide a path for the high-level data signals. The slip rings were mounted on the un-splined portion of the splined shaft. About 0.4 inches was machined off the face of the slip yoke to insure it would not make contact with the slip rings. Figure 6.2 shows photographs of the driveshaft instrumentation assembly.

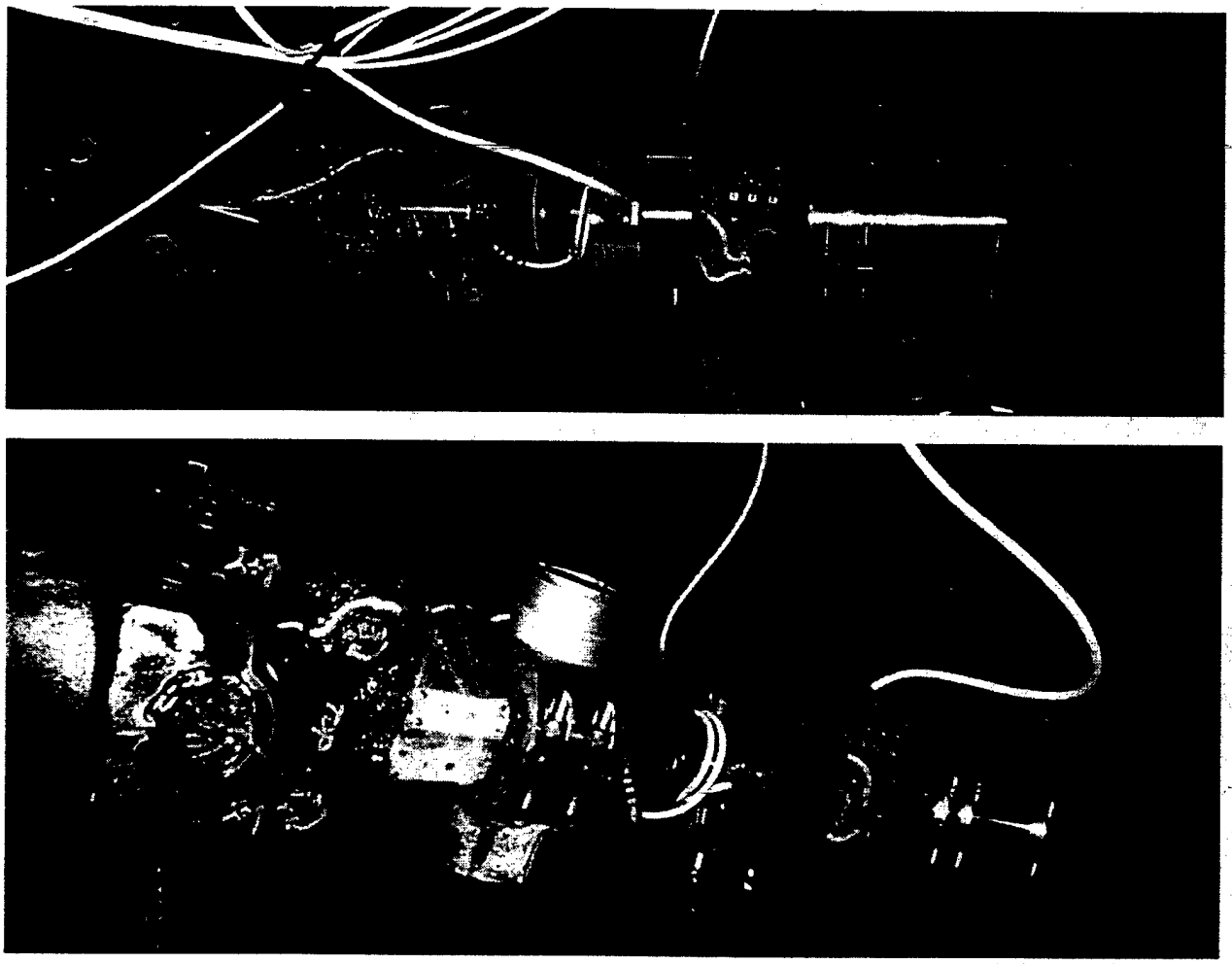

Figure 6.2 Photographs of Instrumented Meritor original production driveshaft

The driveshaft instrumentation assembly was balanced prior to use. The balance speed was 700 RPM and the final unbalance results were 0.46 oz-in at the slip yoke and 0.39 oz-in at the rear yoke. An uninstrumented driveshaft weighs 62 pounds, the weight of the instrumented driveshaft was 71 pounds.

Driveshaft speed was measured via a one pulse per revolution tooth and a passive magnetic pickup sensor. The tooth was attached to the outside diameter of the transfer case yoke flange. The raw magnetic pickup signal was transformed to a voltage proportional to speed with a frequency to voltage converter.

6.4 Instrumentation

Strain Gage Amplifiers

MSC model AMP-SG-U3 amplifiers were used to provide bridge excitation, shunt calibration (span verification), and amplification of the torque, thrust, and bending signals. MSC model AMP-SG-U2-20 amplifiers were used to provide bridge excitation, shunt calibration (span verification), and amplification of the force signals measured at the U-joint. All amplifiers were located on the spinning side of the slip rings and close to the strain gage bridges. This arrangement offers two key advantages: 1) it provides a clean, well regulated bridge voltage supply and 2) data signal return leadwires, including connections across slip rings, carry a high-level signal which improves the signal to noise ratio.

Thermocouple Amplifiers

MSC model AMP-TC2-2 type-K thermocouple conditioning amplifiers were used to condition the thermocouples that sensed temperatures at the U-joint bearing caps. These amplifiers were located on the slip yoke close to the U-joint. This arrangement avoided connecting thermocouple wire across slip rings that can introduce error if the slip ring rotor and stator connections are not the same temperature or if there is variation of contact temperatures within the slip ring assembly.

Power Supply and Control for Spinning Amplifiers

An MSC model PS-DC-1.0V2 DC power supply was used to power all spinning strain gage and thermocouple amplifiers. This unit also invoked shunt calibration (span verification) and removal of bridge excitation for noise checking.

Slip Rings

MSC model B6-2W weatherproof through-bore slip rings were used to conduct power and control signals to the spinning amplifiers as well as provide return paths for high-level data signals. Each slip ring unit had six circuits for a total of twelve. Due to the twelve-circuit limitation, only one of the four thermocouple measurements could be made *simultaneously* with all other driveshaft measurements. The other three thermocouple measurements could be made by simply activating a switch mounted on the driveshaft that swapped three of the driveshaft load measurements for the other three remaining thermocouple signals.

Magnetic Pickup

An Electro model 3015A variable reluctance sensor was used to sense passage of a single tooth on the transfer case yoke flange.

Frequency to Voltage Conversion

An MSC EE-PS series frequency to voltage electronic unit was used to convert the signal from the magnetic pickup to a voltage proportional to frequency.

Data Recorder

A Megadac model 6510DC digital data acquisition unit equipped with AD694SH signal conditioning cards was used to record all test data. Data were recorded on a 500-megabyte/side optical disk. The disk identification number is TACOM FMTV 5A. An index of pertinent datasets recorded on this disk is given in Appendix E. The Megadac Test Control Software (TCS) test name is FMTVCEP*. The data were sampled at 2048 samples/second/channel. All channels of data were anti-alias filtered using the built-in filters of the Megadac AD694SH cards. The cutoff frequencies of the anti-alias filters were set to 200 Hz. The transfer function of these filters is given in Appendix F.

6.5 Presentation and Analysis of the Experimental Data

All experimental test data presented in this section were measured with the rear wheel axles of the vehicle removed. This allowed the driveshaft to be driven by the engine while the vehicle was parked in the laboratory. Consequently, no torque load was placed on the driveshaft other than that due to friction and inertial loads. Recall that all driveshaft transducer signals were balanced (zeroed) with the rotating coordinate system (as marked on the driveshaft) aligned with SAE vehicle coordinate directions. The polarities are defined in section 6.3.

The data presented here were recorded on October 23, 1998 at the Michigan Scientific Corporation laboratory in Milford, MI.

The test consisted of sweeping the driveshaft speed from zero RPM to approximately 2900 RPM (equivalent to about 48 mph road speed, i.e. one driveshaft rev./second ≈ one mph road speed) and back to zero RPM. The duration of the test run was about three minutes. Prior to the test a spline joint "hinging" measurement as described in Appendix G was made. Also measured were pre- and post-test indicated driveshaft run-outs. These results are contained in Appendix C.

Time histories of the data are shown in figures 6.3 through 6.5. Each figure contains the driveshaft speed signal for reference. Please note that due to signal drop-out, ***the driveshaft speed signal is only valid in the time range of about 125 to 165 seconds.*** Fortunately, this is the relevant time period of the test. Figures 6.6 through 6.11 are successive zoom-ins of this time period. Recall when examining these figures that the load data are measured with respect to a rotating coordinate system. Vector-sum magnitudes of the bending moments and U-joint forces from 144 to 164 seconds are given in figure 6.12. Notice the increase of the magnitude at time equal to ≈154 seconds. This corresponds to a driveshaft speed of 2930 RPM (49 Hz 1st order) which corresponds to a road speed of about 50 mph. As stated in section 5.7.4, it is important to understand that the critical speed of the instrumented driveshaft is lowered by the added mass of the instrumentation. This mass was also added to the computer model for correlation of computed and measured dynamic responses.

* Other channels of data beyond the scope of this section of the report are also included in this TCS test.

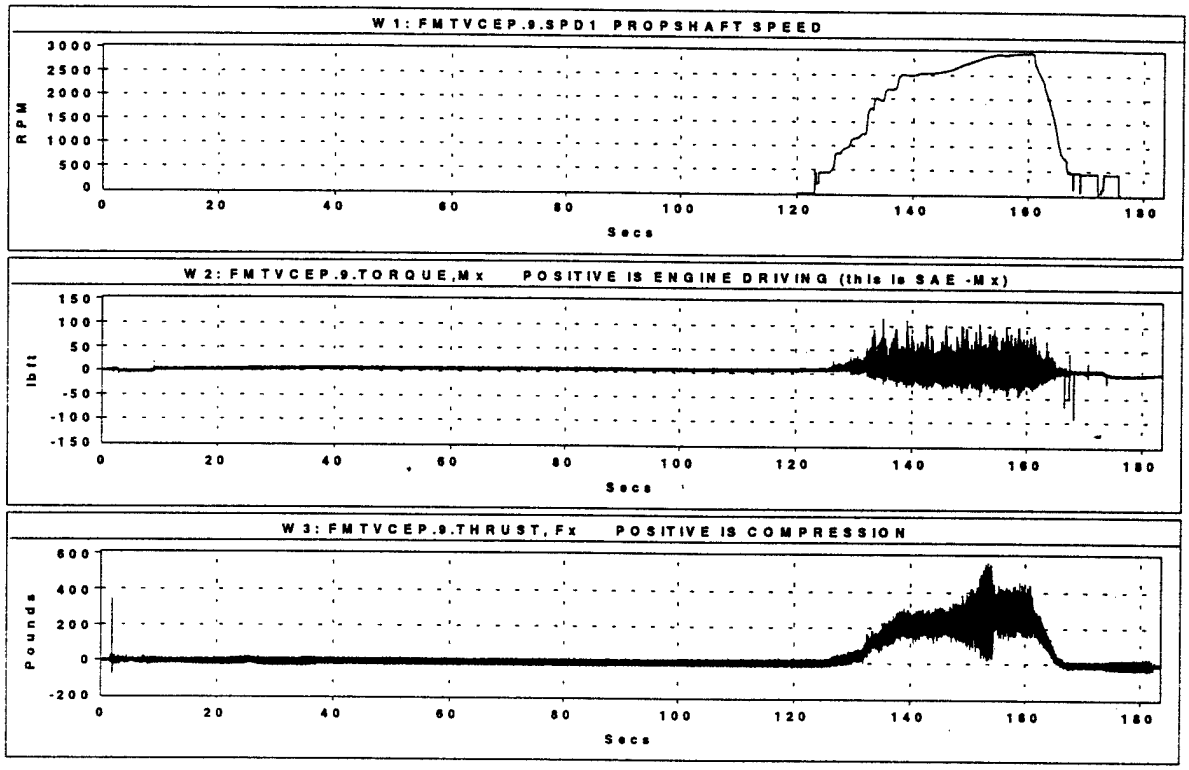

Figure 6.3 Time history data from instrumented Meritor original production driveshaft

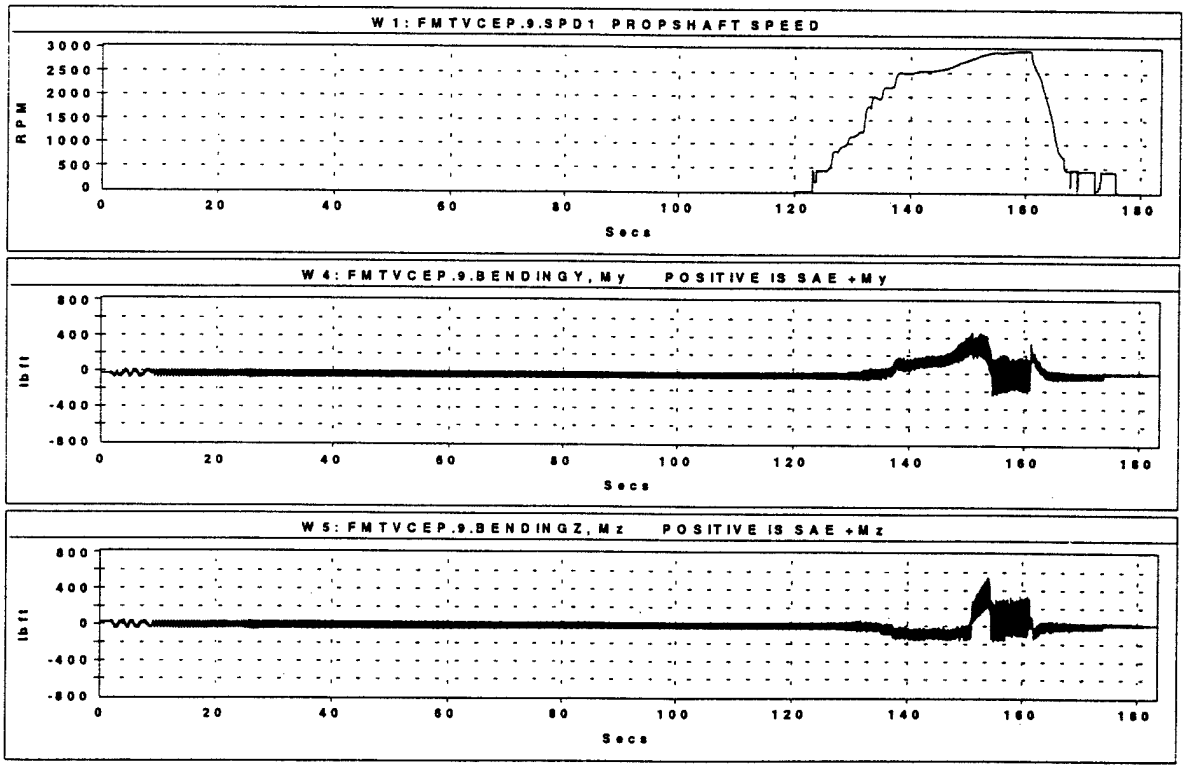

Figure 6.4 Time history data from instrumented Meritor original production driveshaft

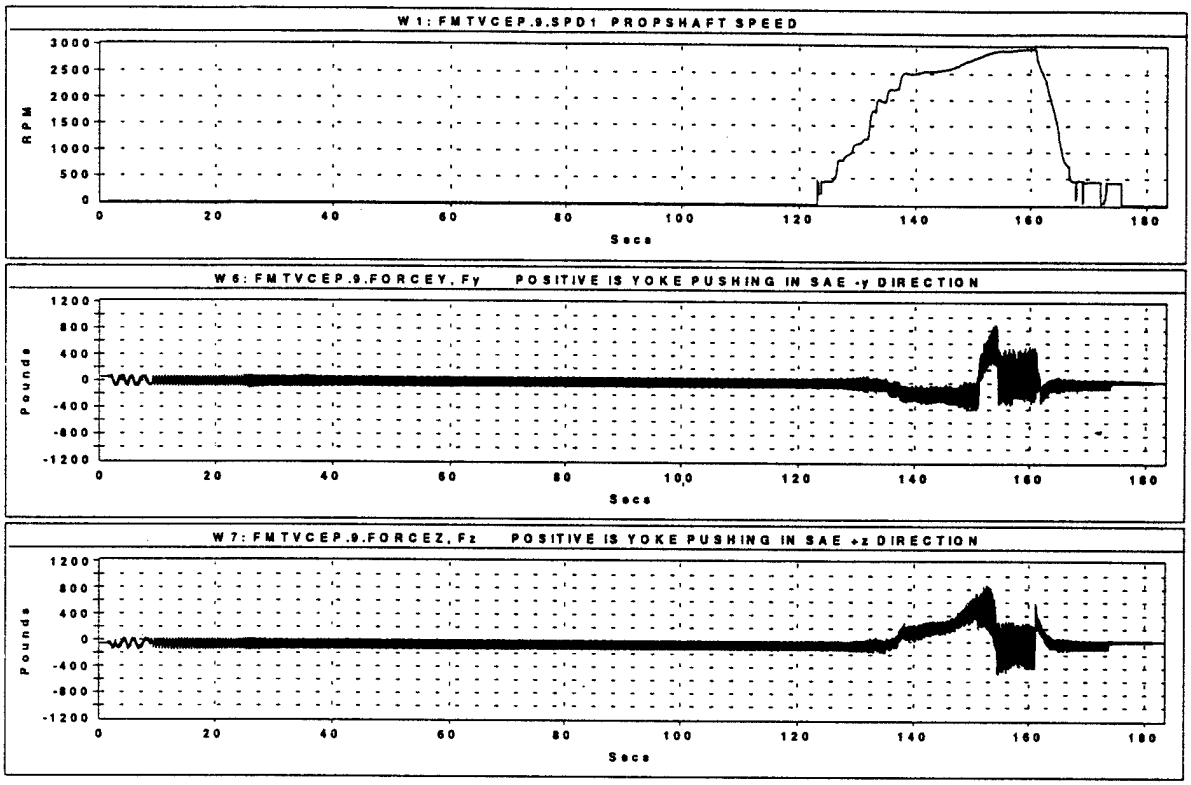

Figure 6.5 Time history data from instrumented Meritor original production driveshaft

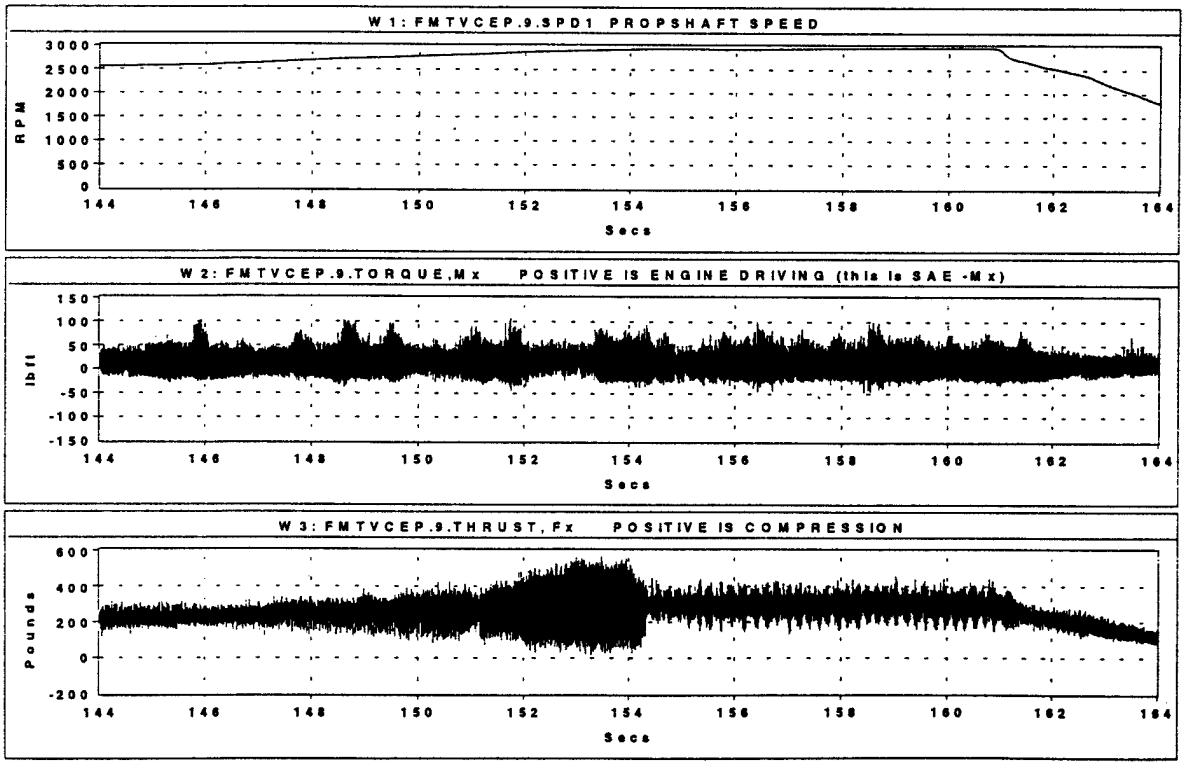

Figure 6.6 Time history data from instrumented Meritor original production driveshaft

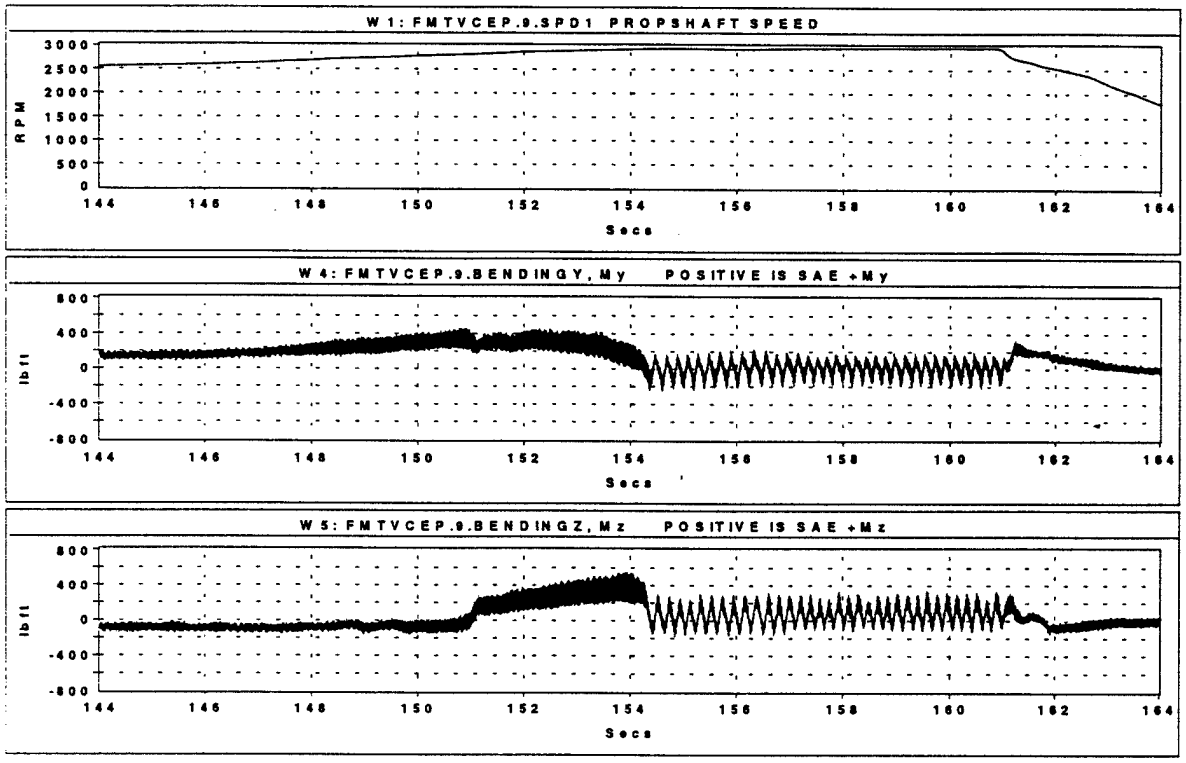

Figure 6.7 Time history data from instrumented Meritor original production driveshaft

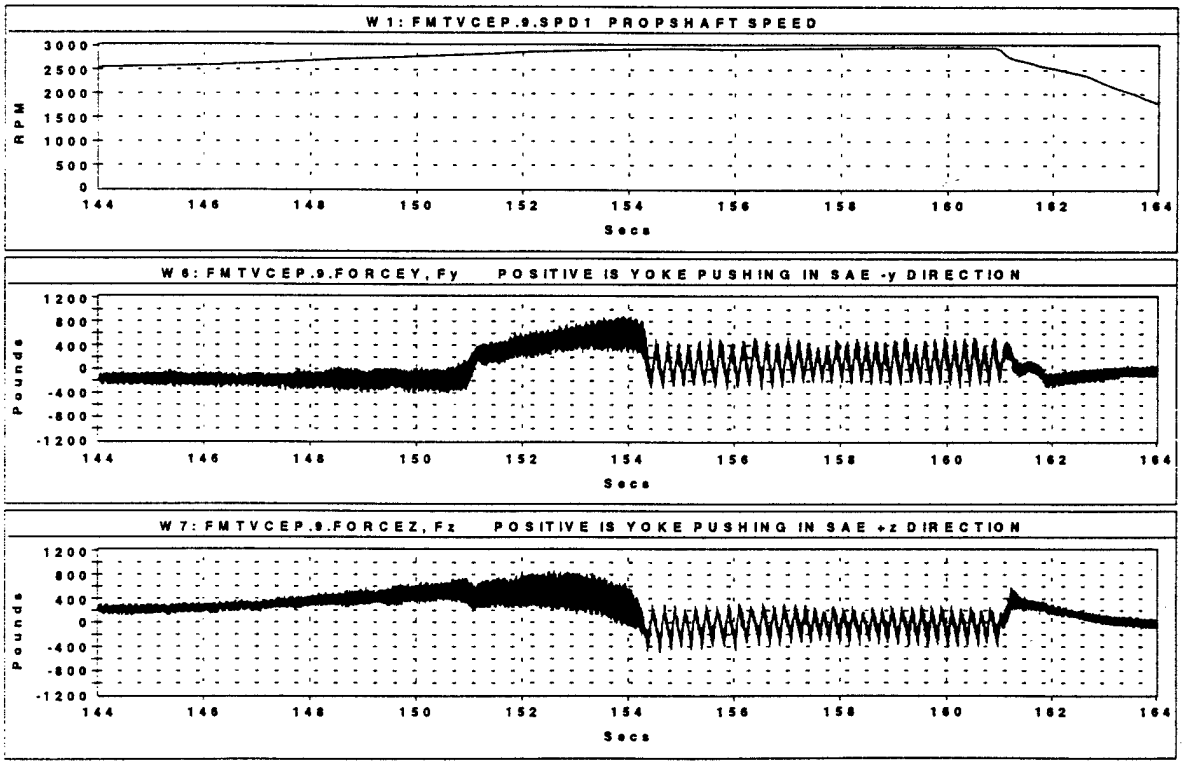

Figure 6.8 Time history data from instrumented Meritor original production driveshaft

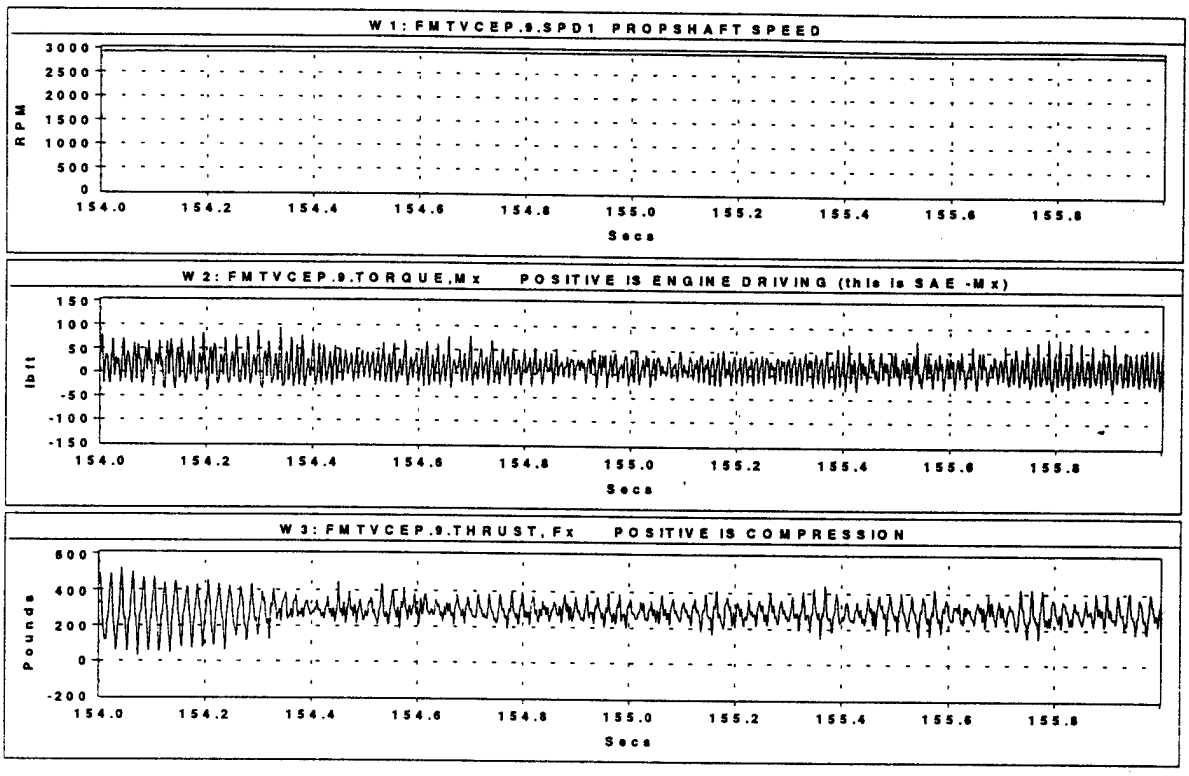

Figure 6.9 Time history data from instrumented Meritor original production driveshaft

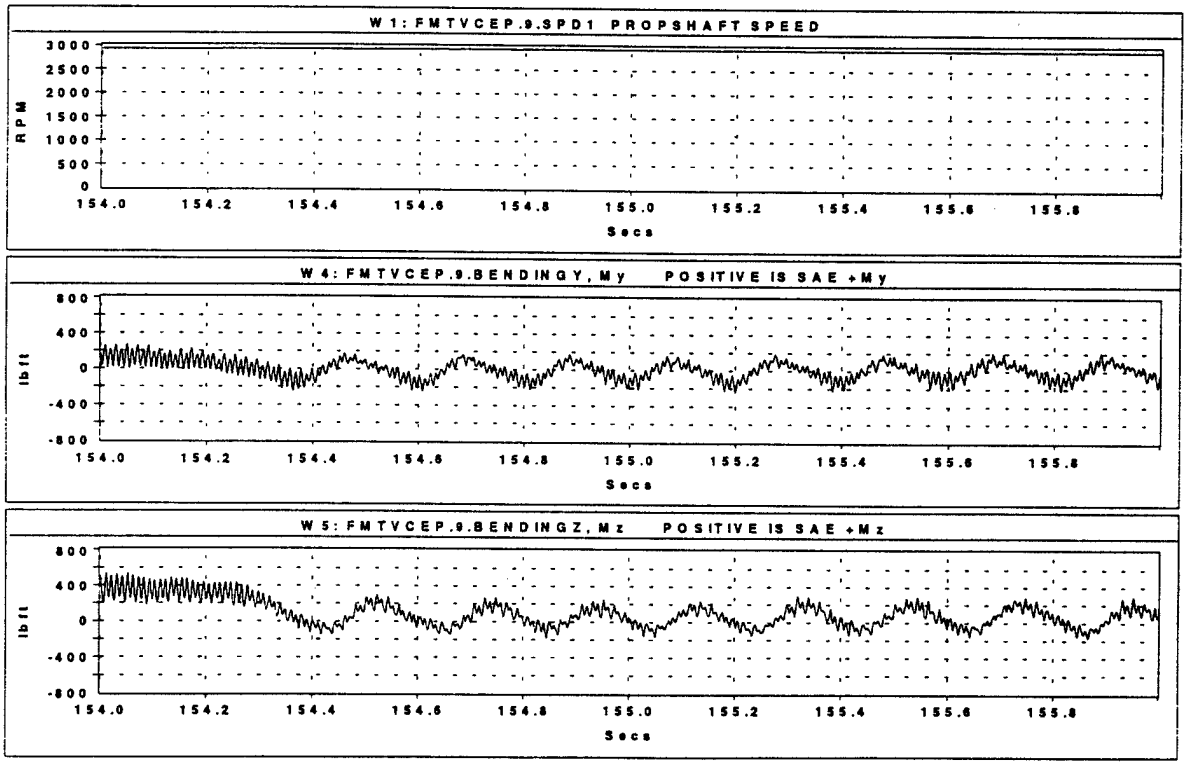

Figure 6.10 Time history data from instrumented Meritor original production driveshaft

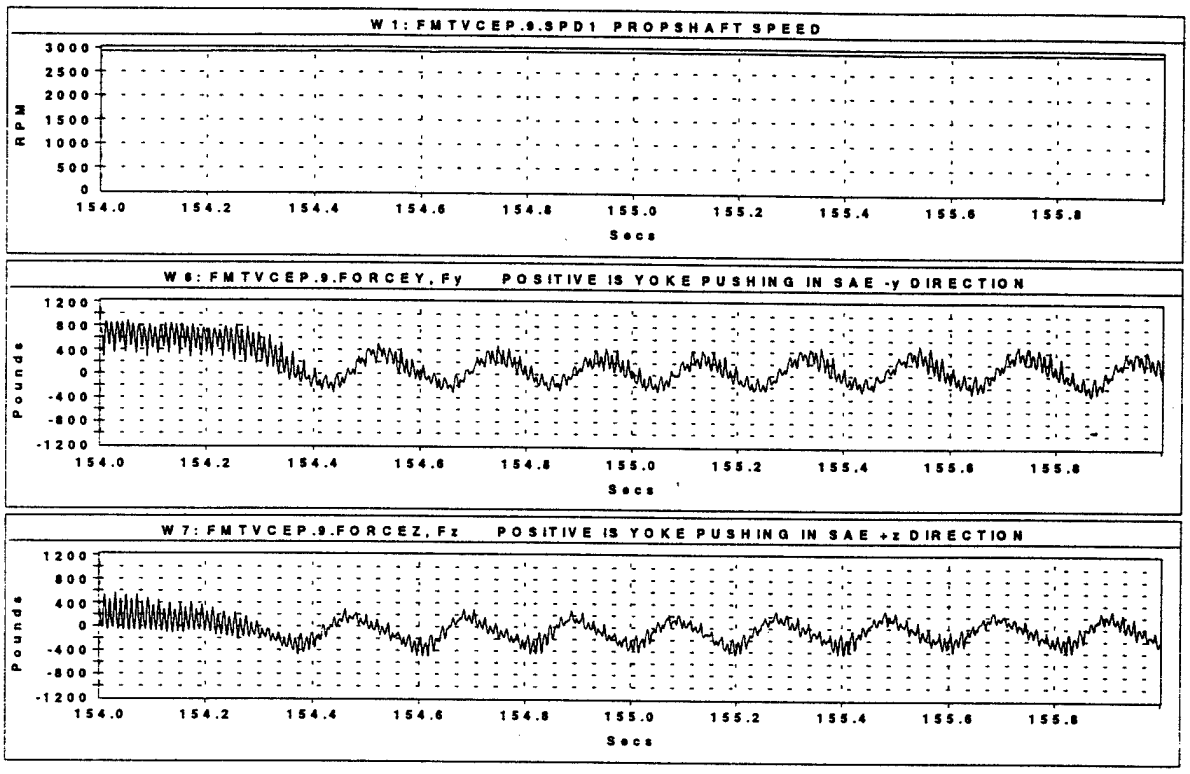

Figure 6.11 Time history data from instrumented Meritor original production driveshaft

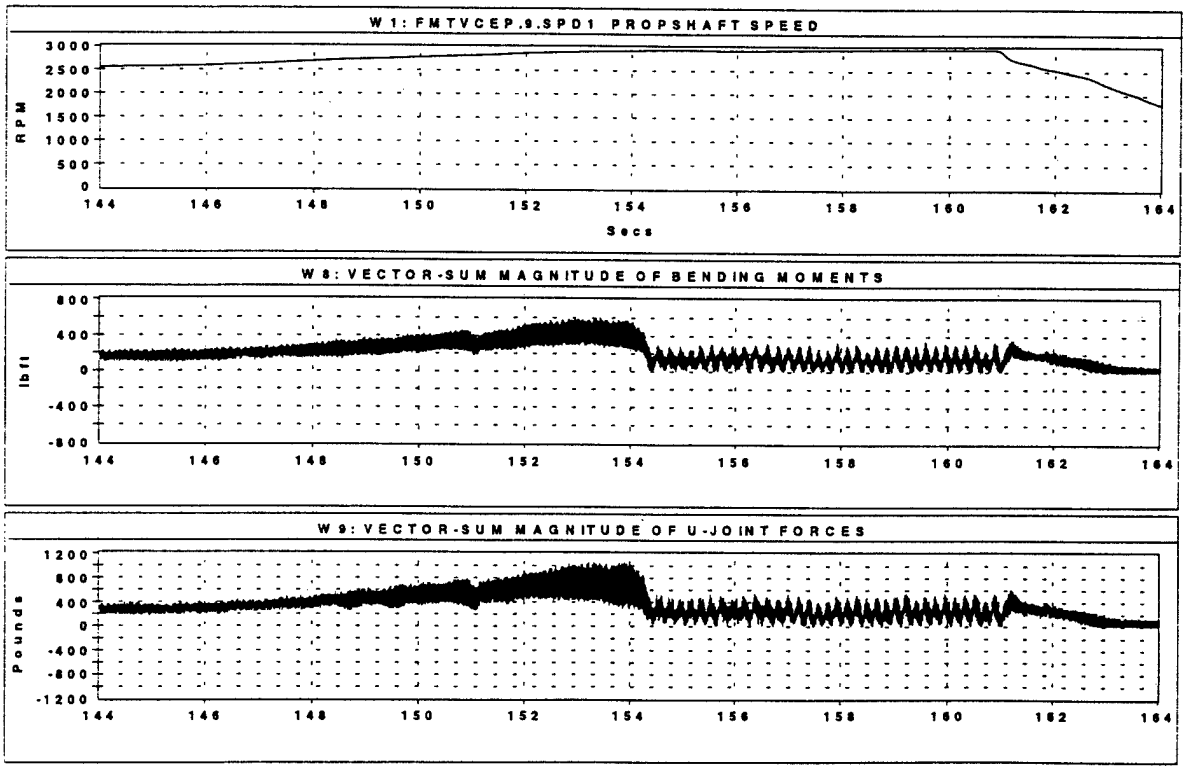

Figure 6.12 Time history data from instrumented Meritor original production driveshaft

Because the time history data are measured with respect to a rotating coordinate system it is difficult to intuitively understand the dynamic forces that are imposed upon the non-rotating transfer case and axle housing at the ends of the driveshaft. To aid in the understanding, the bending moment and U-joint force data were mathematically manipulated to transform them into time histories with respect to a non-rotating coordinate system. The manipulation can be described by referring to figure 6.13. The driveshaft speed data (window W1 at the top of the figure) is first converted from units of RPM to units of radians/second (window W10). This result is then mathematically integrated to obtain displacement in radians (window W11). The next step is to perform sine and cosine functions on the displacement (this is shown in windows W12 and W13 respectively). Once these sine and cosine results are available, the standard formulas for coordinate transformation can be implemented. It must be stated that this technique does not reveal *absolute* displacement of the driveshaft, i.e. we do not know the starting point of the rotational driveshaft displacement relative to stationary vehicle coordinates. This is due to the unknown start of the integration*. This does not however prohibit performing the transformation and although the orientation of the *new non-rotating* coordinate system with respect to vehicle coordinates is unknown, the transformation still provides insight.

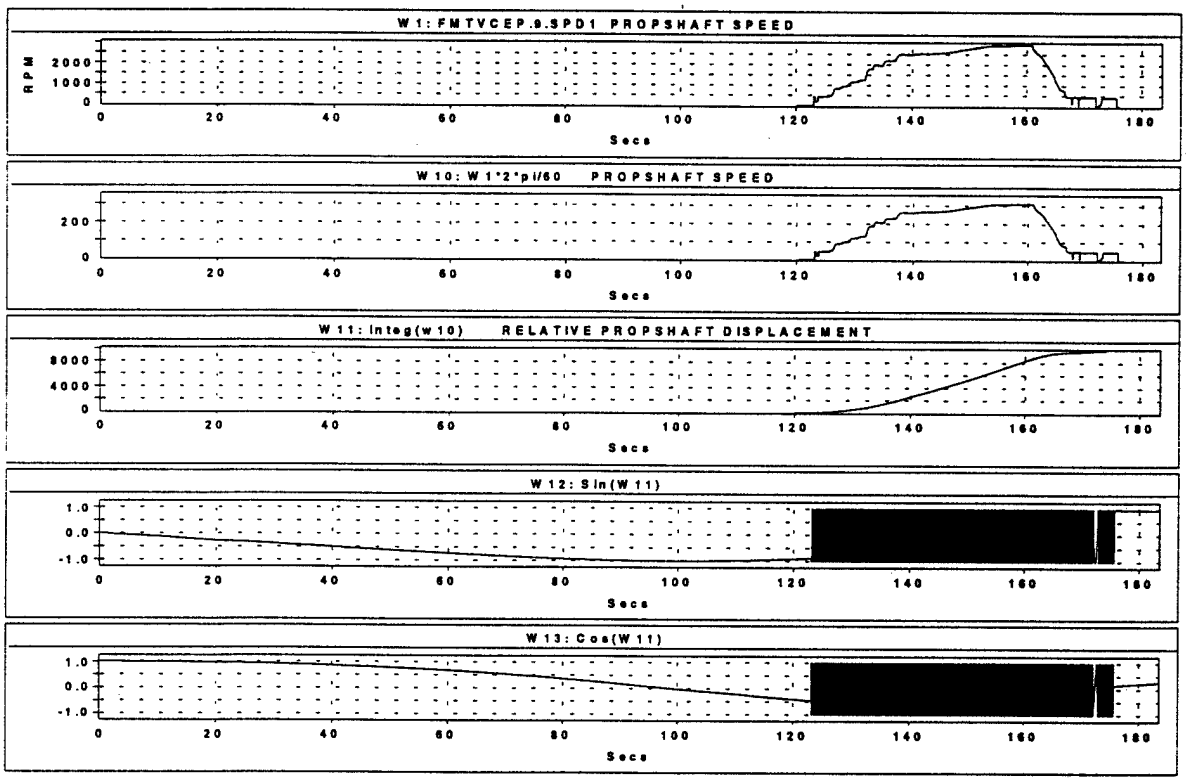

Figure 6.13 Manipulation algorithm to transform data from a rotating to a stationary coordinate system

The results of the transformation are shown in figures 6.14 through 6.18. These figures have the same layout and scaling as figures 6.7, 6.8, 6.10, 6.11, and 6.12 in order to assist in comparing rotating to non-rotating coordinate system data. As expected, the vector-sum magnitudes of each system are equivalent. Note that the transformed data are now composed primarily of 1st order frequency content with a mean approximately equal to zero.

* A once per revolution index pulse was not available for use as a reference to start the integration. Also, integration over the "drop-out" portion of the driveshaft speed signal is of no concern since we recognize that absolute displacement is not obtainable.

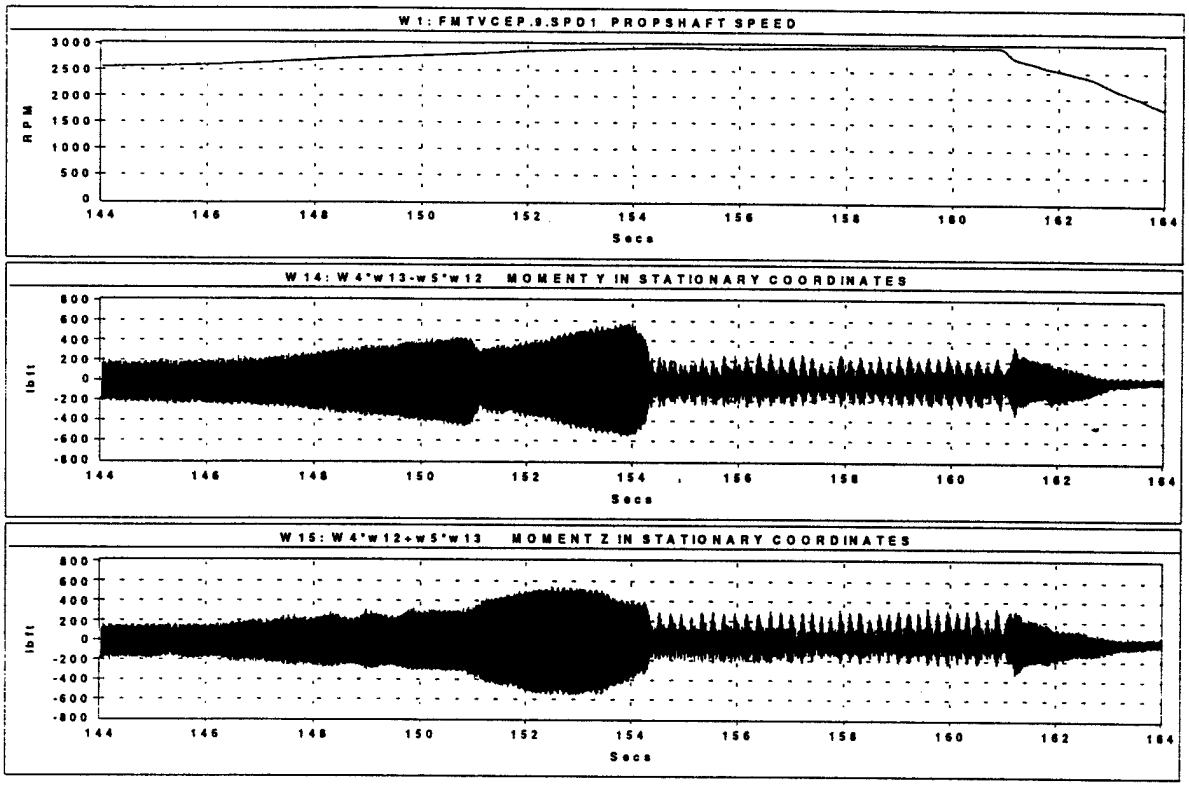

Figure 6.14 Time history data from instrumented Meritor original production driveshaft in stationary coordinate system

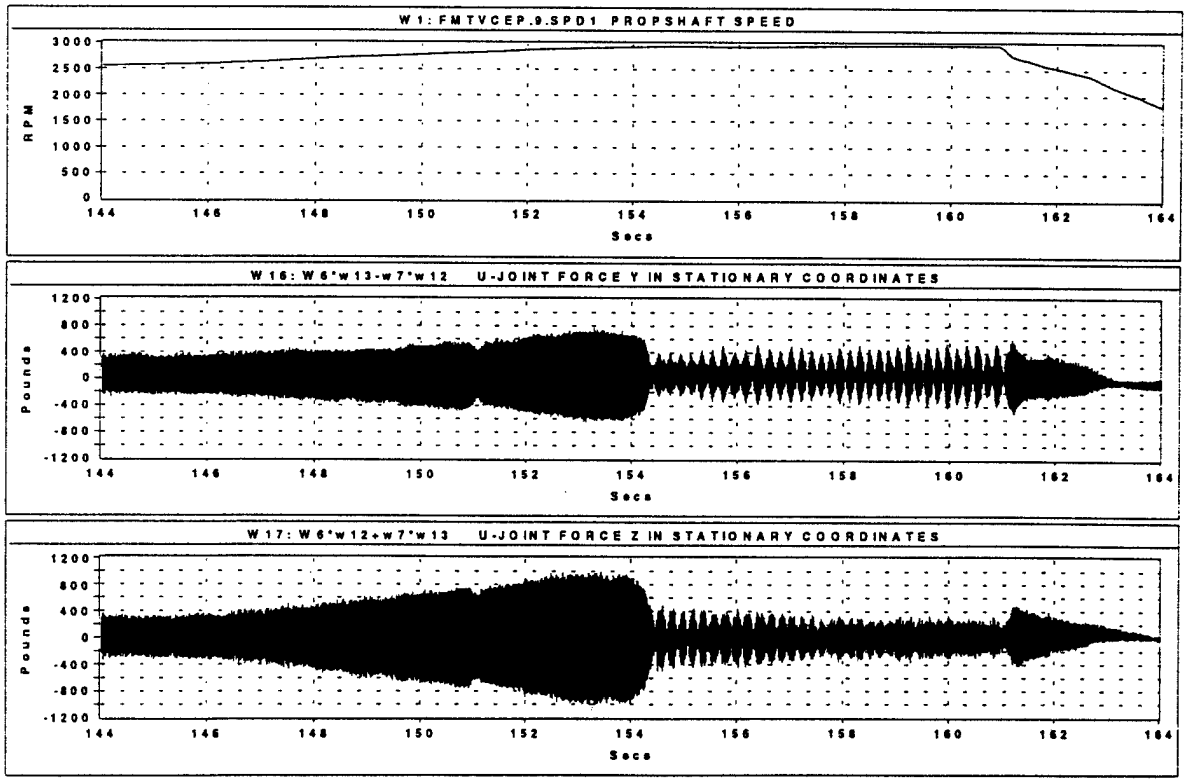

Figure 6.15 Time history data from instrumented Meritor original production driveshaft in stationary coordinate system

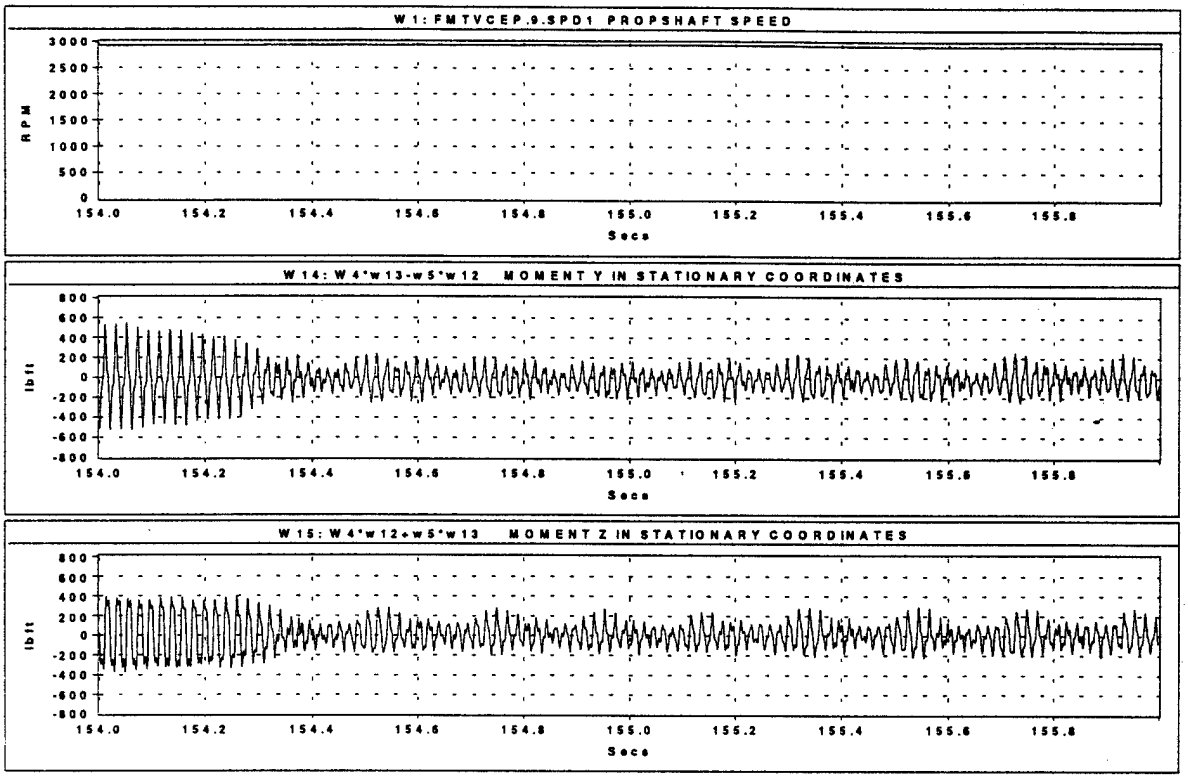

Figure 6.16 Time history data from instrumented Meritor original production driveshaft in stationary coordinate system

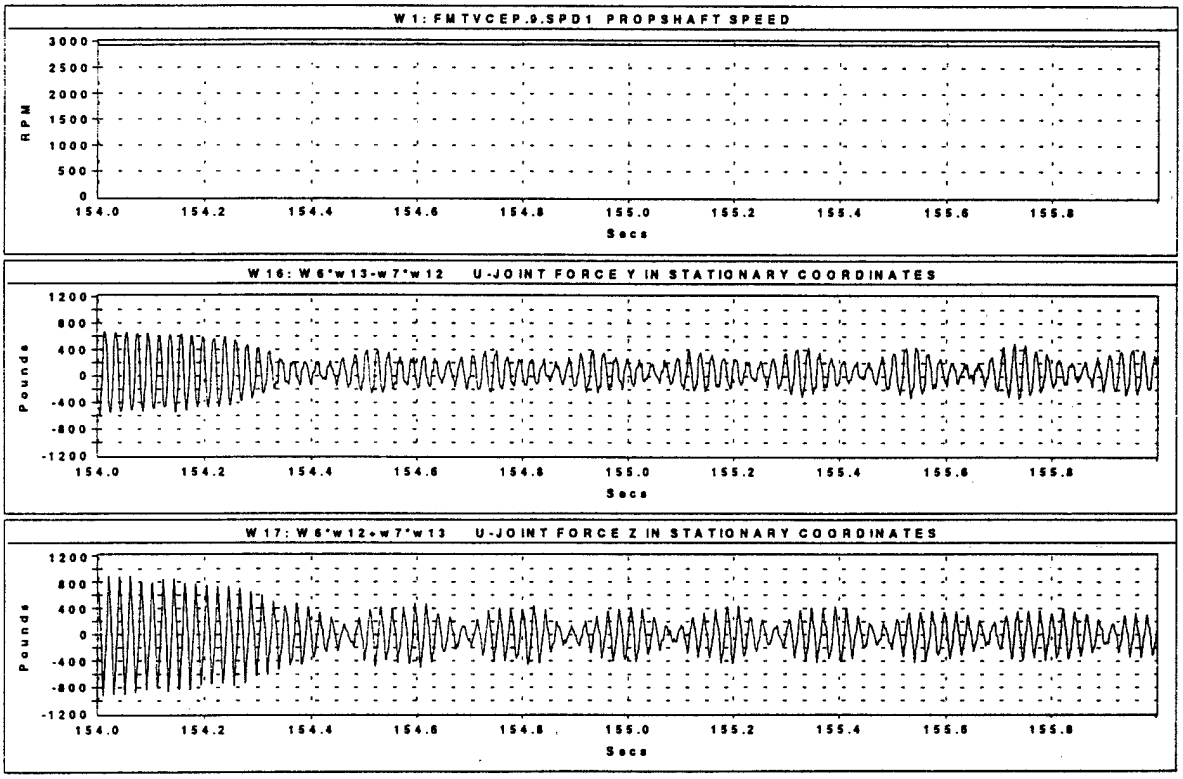

Figure 6.17 Time history data from Instrumented Meritor original production driveshaft in stationary coordinate system

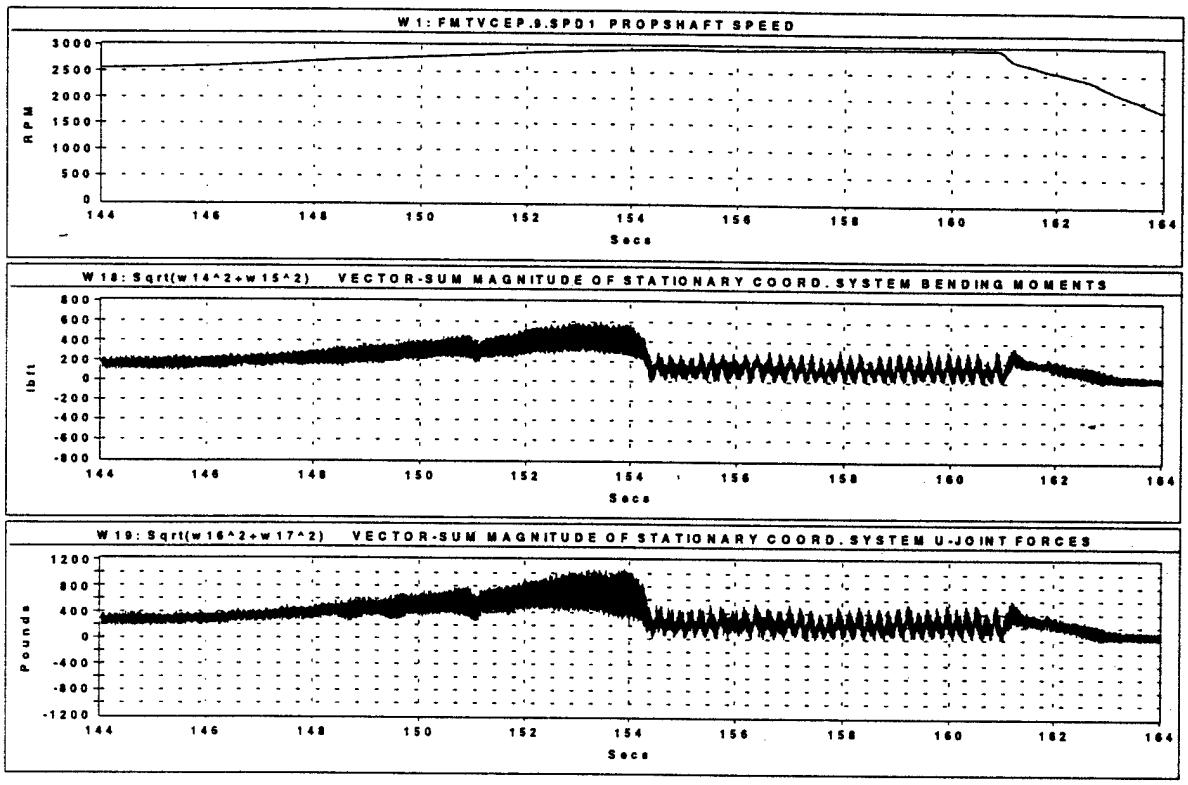

Figure 6.18 Time history data from Instrumented Meritor original production driveshaft in stationary coordinate system

Figure 6.19 is an "XY" plot of the transformed U-joint force data over the time period 154 to 155 seconds. The trace of this plot describes the path of the tip of a radial force vector rotating with the driveshaft as observed by a stationary observer. As alluded to above, the orientation of this plot with respect to vehicle coordinates is unknown.

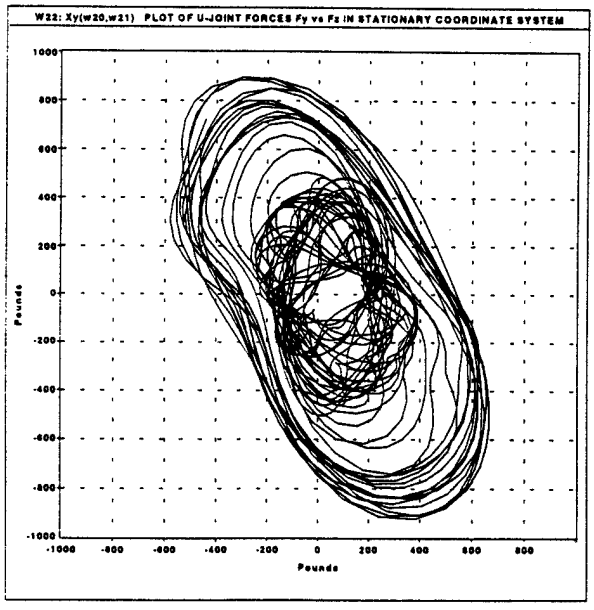

Figure 6.19 "XY" plot of U-joint forces imposed upon transfer case rear output housing over period 154 to 155 seconds (instrumented Meritor original production driveshaft)

APPENDICES

APPENDIX A

EXPERIMENTAL MEASUREMENT OF LATERAL AND VERTICAL POWERPACK BENDING STIFFNESS

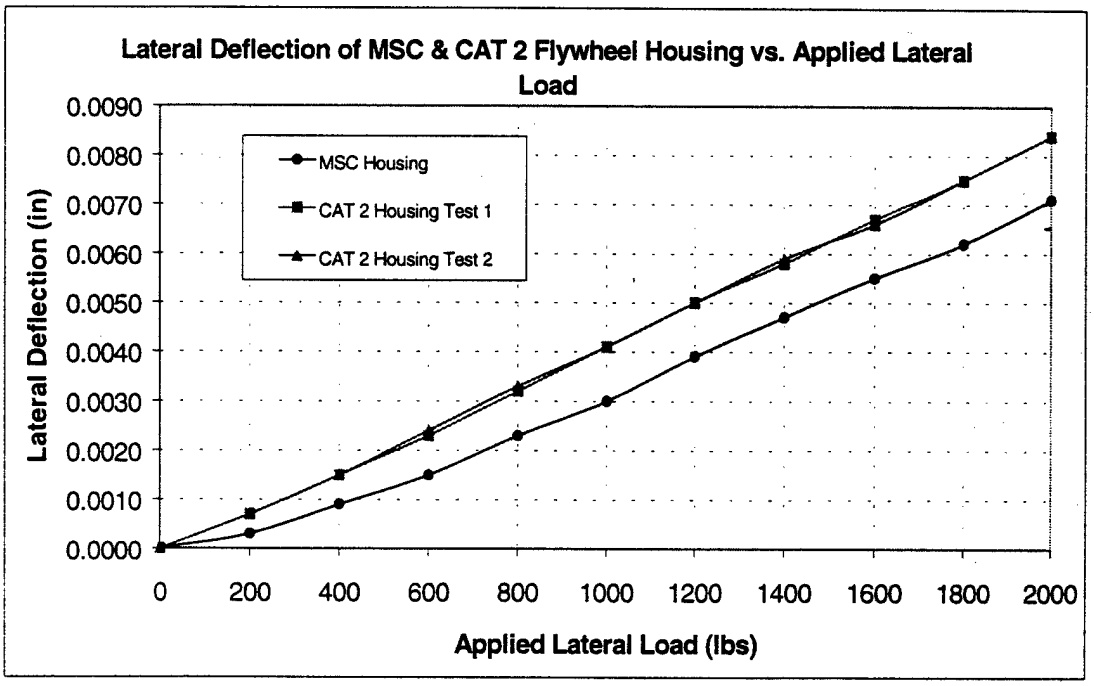

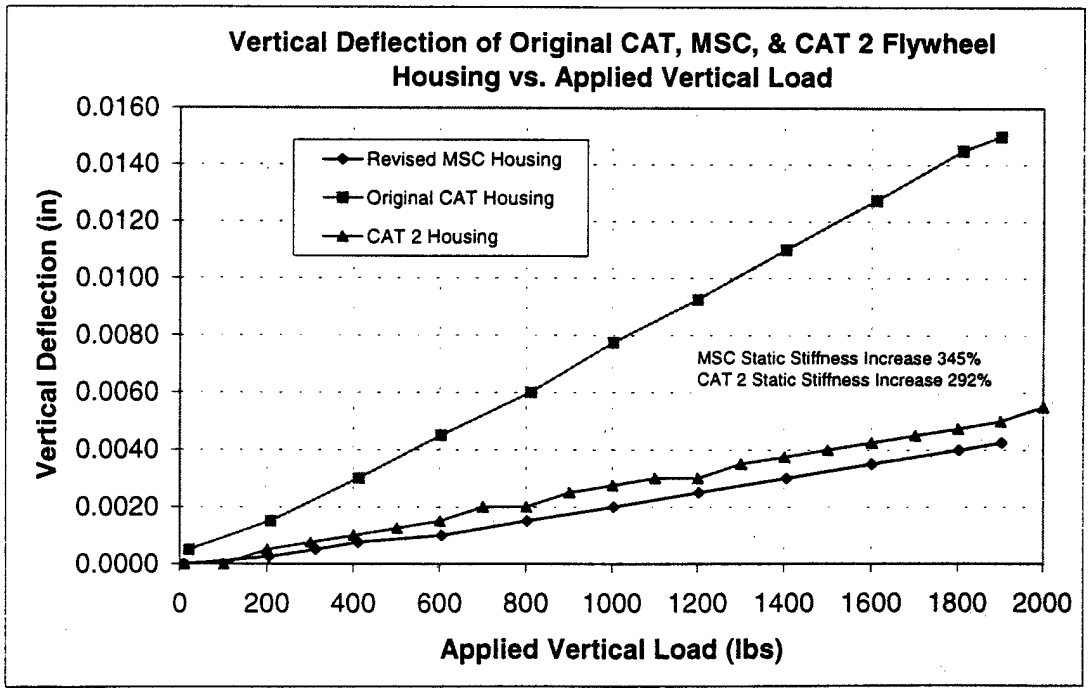

APPENDIX A

EXPERIMENTAL MEASUREMENT OF LATERAL AND VERTICAL POWERPACK BENDING STIFFNESS

8-29-98

VERTICAL BENDING STIFFNESS CALCULATION FOR MSC HOUSING

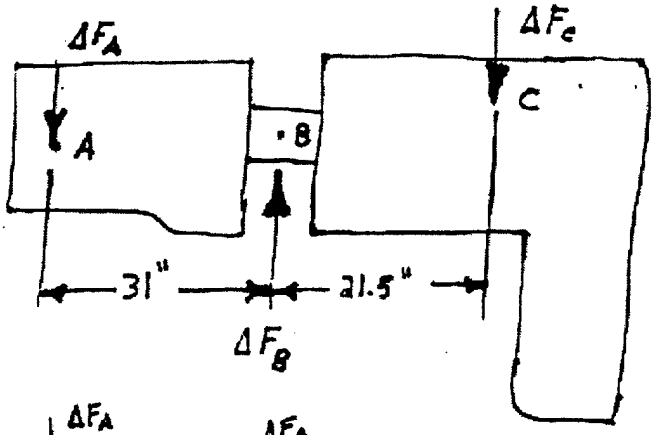

$+\circlearrowleft \Sigma M_A = 0;$

$\Delta F_B\ 31 - \Delta F_C\ 52.5 = 0$

$\Delta F_C = \Delta F_B \left(\frac{31}{52.5}\right)$

$\Delta F_C = \Delta F_B\ (.590)$

$+\uparrow \Sigma F_z = 0;$

$-\Delta F_A + \Delta F_B - \Delta F_C = 0$

$\Delta F_A = \Delta F_B\ (1 - .590)$

$\Delta F_A = \Delta F_B\ (.410)$

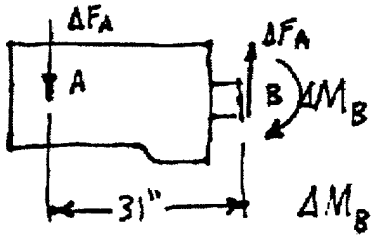

$\Delta M_B = \Delta F_A(31) = \Delta F_B(.410)\ 31$

$\Delta M_B = 1000(.41)(31) = 12{,}695\ \text{in·lb}$

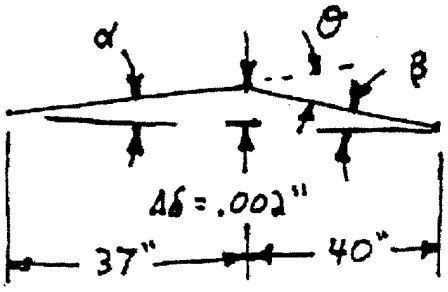

$\alpha = \tan^{-1}\left(\frac{.002}{37}\right) = 5.41 \times 10^{-5}\ \text{rad}$

$\beta = \tan^{-1}\left(\frac{.002}{40}\right) = 5.00 \times 10^{-5}\ \text{rad}$

$\theta = \alpha + \beta = 1.041 \times 10^{-4}\ \text{rad}$

VERTICAL BENDING STIFFNESS = K_Y

$$K_Y = \frac{\Delta M_B}{\theta} = \frac{12695}{1.041 \times 10^{-4}} = 122.00 \times 10^6\ \frac{\text{in·lb}}{\text{rad}}$$

EJM

APPENDIX A

EXPERIMENTAL MEASUREMENT OF LATERAL AND VERTICAL POWERPACK BENDING STIFFNESS

9-8-98

LATERAL BENDING STIFFNESS CALCULATION FOR MSC HOUSING

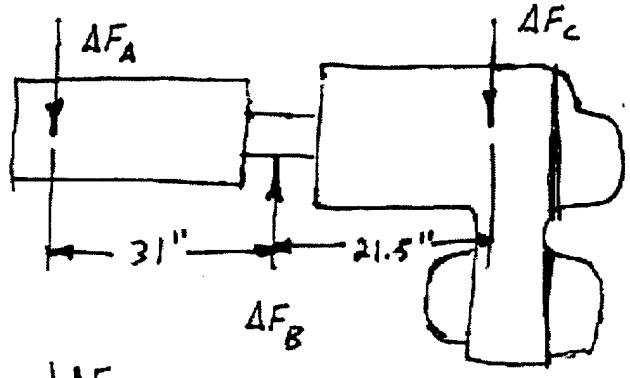

$+\circlearrowleft \Sigma M_A = 0;$

$\Delta F_B\, 31 - \Delta F_C\, 52.5 = 0$

$\Delta F_C = \Delta F_B \left(\frac{31}{52.5}\right)$

$\Delta F_C = \Delta F_B\,(.590)$

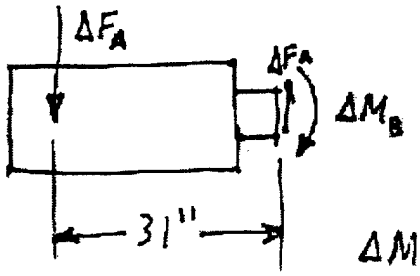

$+\uparrow \Sigma F_V = 0;$

$-\Delta F_A + \Delta F_B - \Delta F_C = 0$

$\Delta F_A = \Delta F_B\,(.410)$

$\Delta M_B = \Delta F_A\, 31 = \Delta F_B\,(.410)\, 31$

$\Delta M_B = 1000\,(.410)\, 31 = 12695$ in-lb

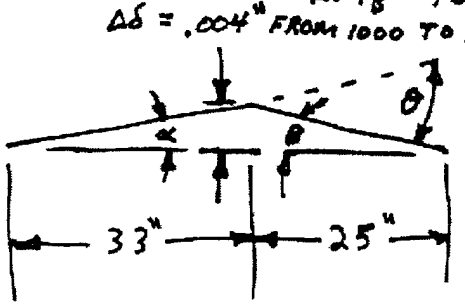

$\alpha = \tan^{-1}\left(\frac{.004}{33}\right) = 1.24\times10^{-4}$ rad

$\beta = \tan^{-1}\left(\frac{.004}{25}\right) = 1.64\times10^{-4}$ rad

$\theta = \alpha + \beta = 2.88\times10^{-4}$ rad

LATERAL BENDING STIFFNESS = K_Z

$$K_Z = \frac{\Delta M_B}{\theta} = \frac{12695}{2.88\times10^{-4}} = 44.04\times10^6 \frac{\text{in-lb}}{\text{rad}}$$

EJM

APPENDIX B

EXPERIMENTAL MEASUREMENTS OF DRIVESHAFT HINGE STIFFNESS FOR MERITOR "ORIGINAL PRODUCTION" AND "A1" DRIVESHAFTS

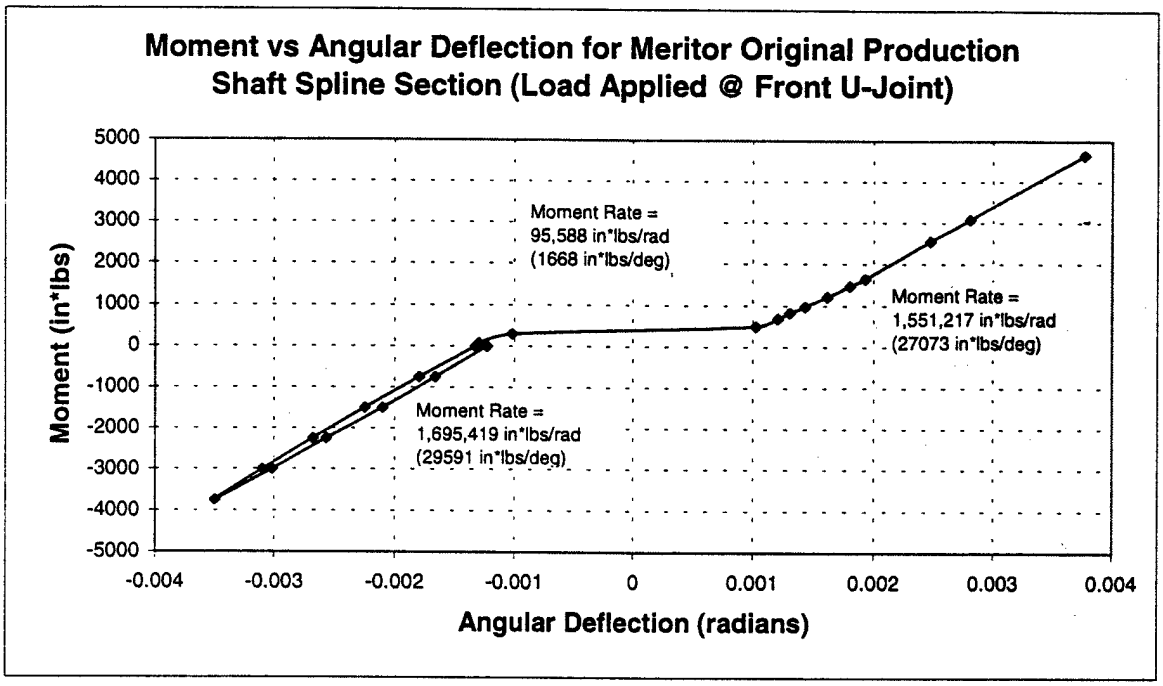

Note: Original factory shaft had 0.027 inch "hinging"

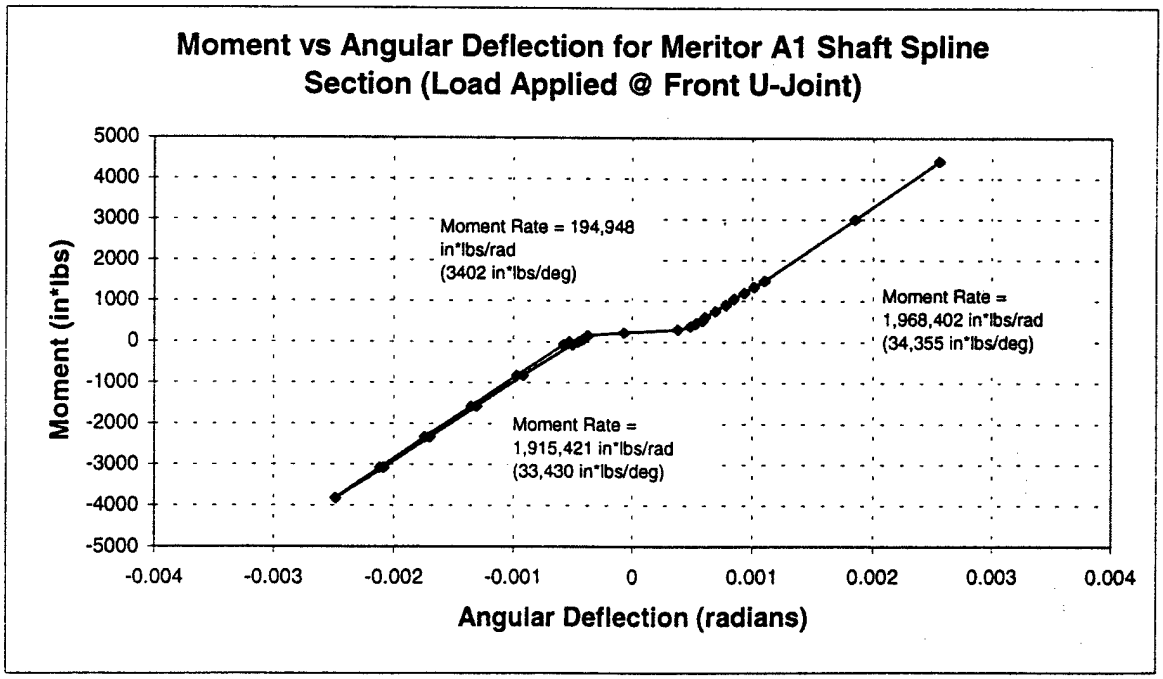

Note: A1 shaft had 0.007 inch "hinging"

APPENDIX C

Pre– and Post–test Run–out Measurements of Instrumented Propshaft
Test Vehicle s/n: AT0357B–AC

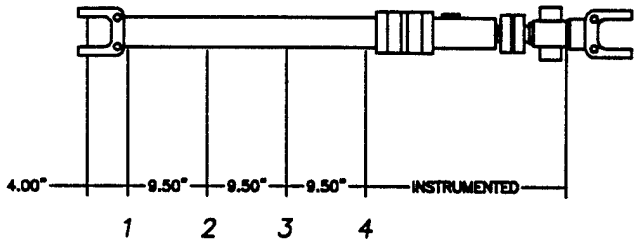

Pre–test Run–out

Location	*Run–out*
(1)	*0.0210"*
(2)	*0.0250"*
(3)	*0.0335"*
(4)	*0.0285"*

Note: Pre–test run–out high points are not co–linear with respect to a fore/aft axis

Post–test Run–out

Location	*Run–out*
(1)	*0.0220"*
(2)	*0.0425"*
(3)	*0.0530"*
(4)	*0.0520"*

Note: Post–test run–out high points are co–linear with respect to a fore/aft axis

Mike Bellaire
12/29/98

APPENDIX D

TRANSFER CASE REAR OUTPUT YOKE STIFFNESS MEASUREMENT

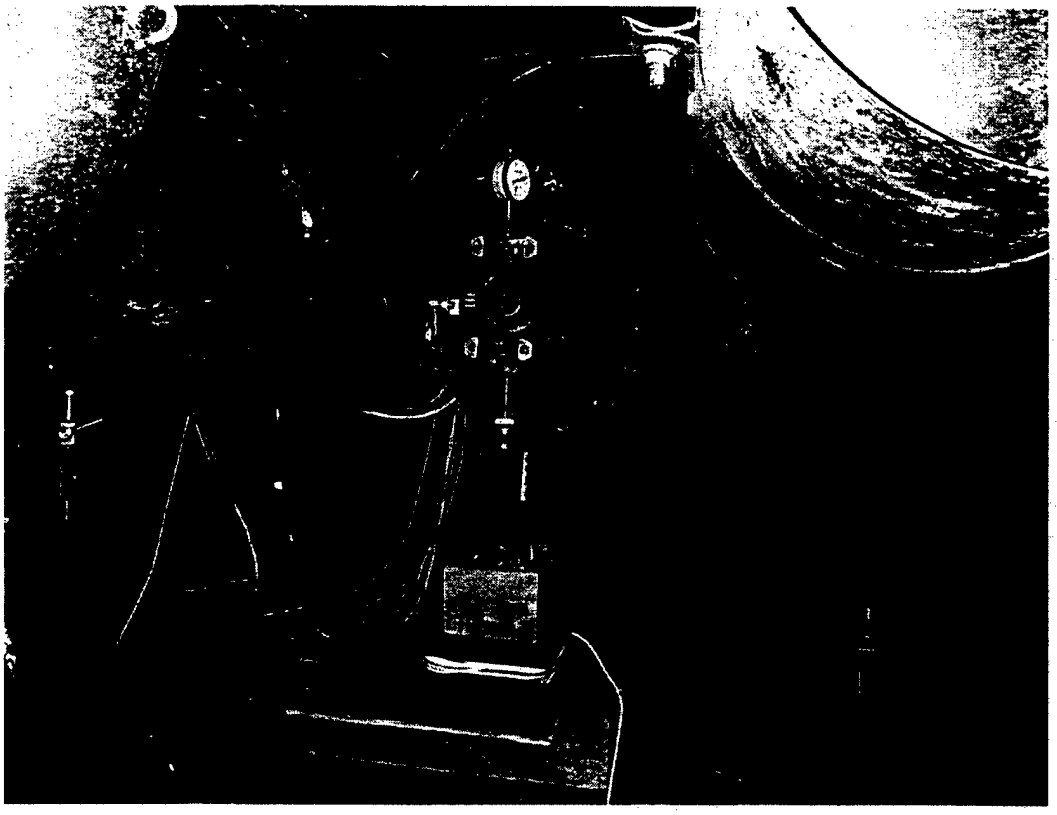

Photograph of setup for measuring transfer case bell housing stiffness at output yoke

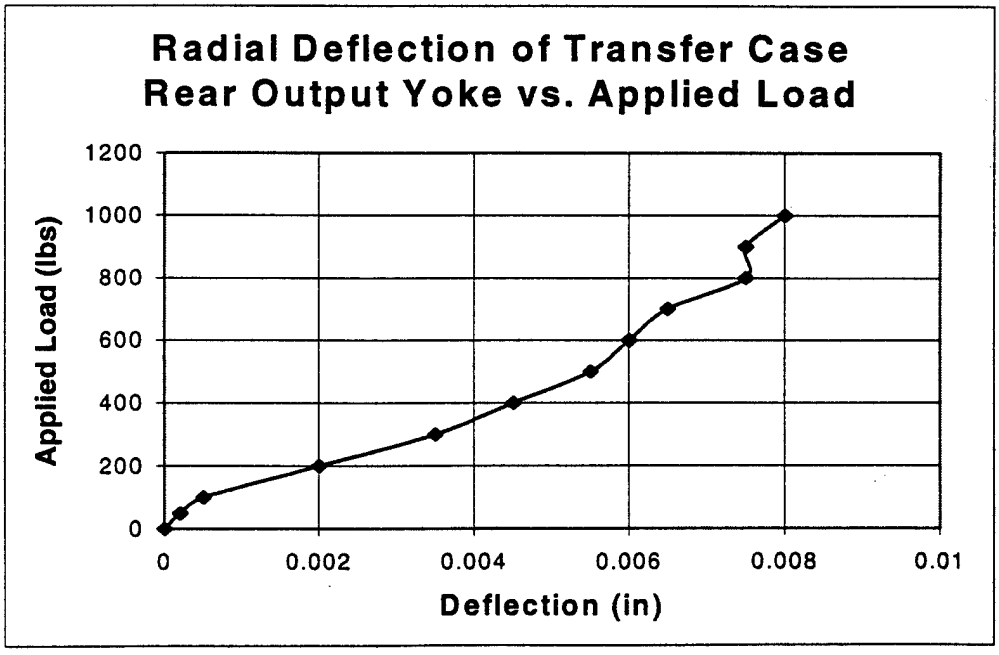

APPENDIX F

TRANSFER FUNCTION OF MEGADAC ANTI-ALIAS FILTERS

BELOW IS THE AMPLITUDE PORTION OF THE TRANSFER FUNCTION OF THE ANTI-ALIAS FILTER OF MEGADAC 684/694 CARDS

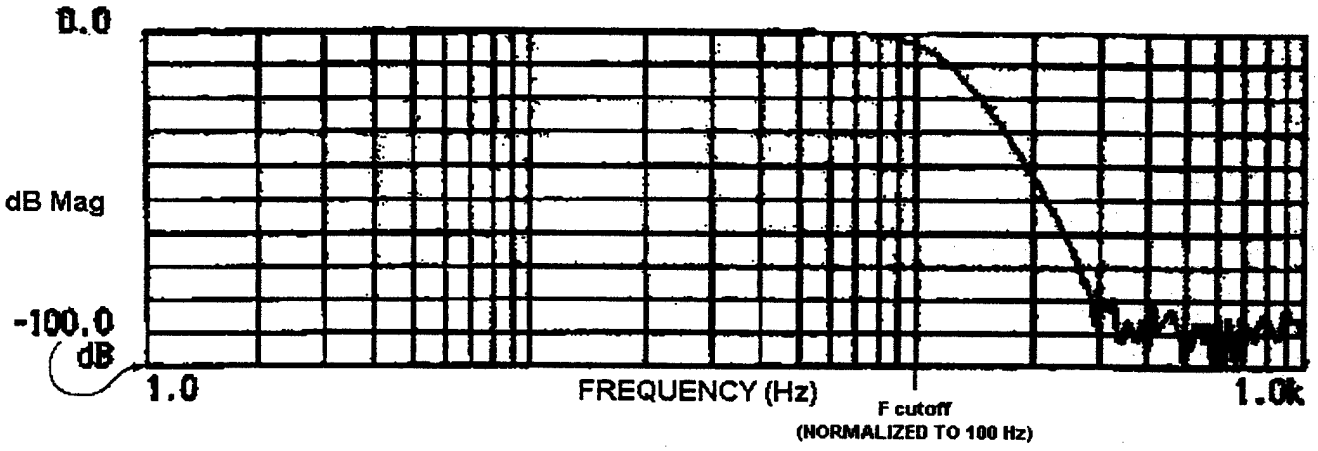

BELOW IS A PLOT OF THE PHASE PORTION OF THE TRANSFER FUNCTION OF THE ANTI-ALIAS FILTER IN THE MEGADAC 684/694 CARDS. THIS PLOT IS BASED UPON THE PHASE VS LOGARITHMIC FREQUENCY PLOT SUPPLIED BY OPTIM. THE POINTS WERE HANDPICKED BY EYE.

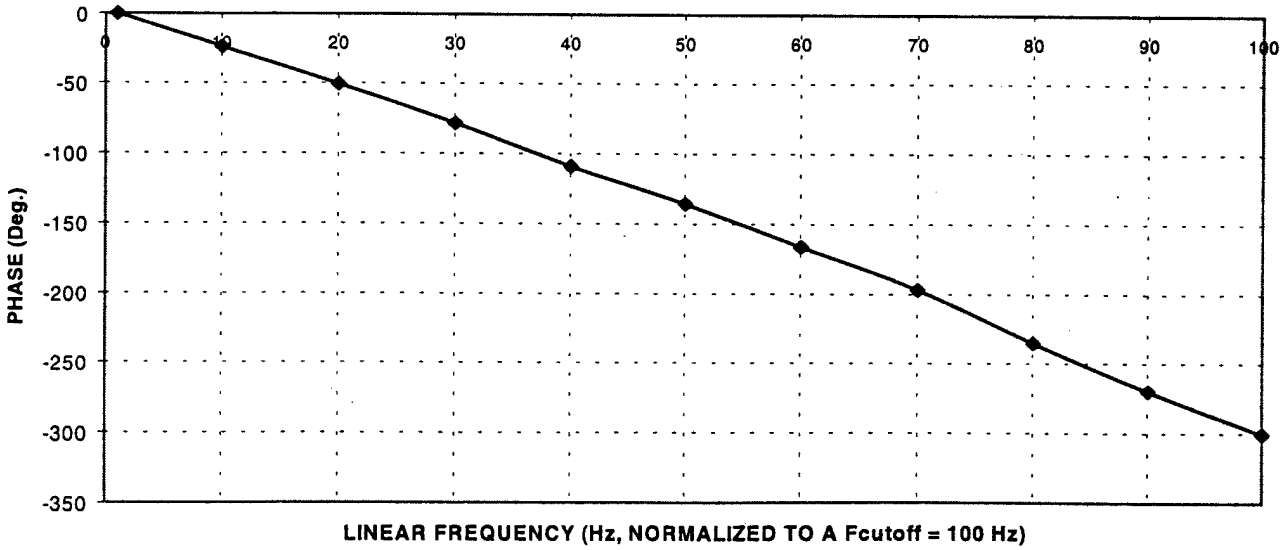

APPENDIX G

SPLINE JOINT HINGE LASH MEASUREMENT SETUP FOR INSTRUMENTED MERITOR ORIGINAL PRODUCTION DRIVESHAFT (PRE-TEST)

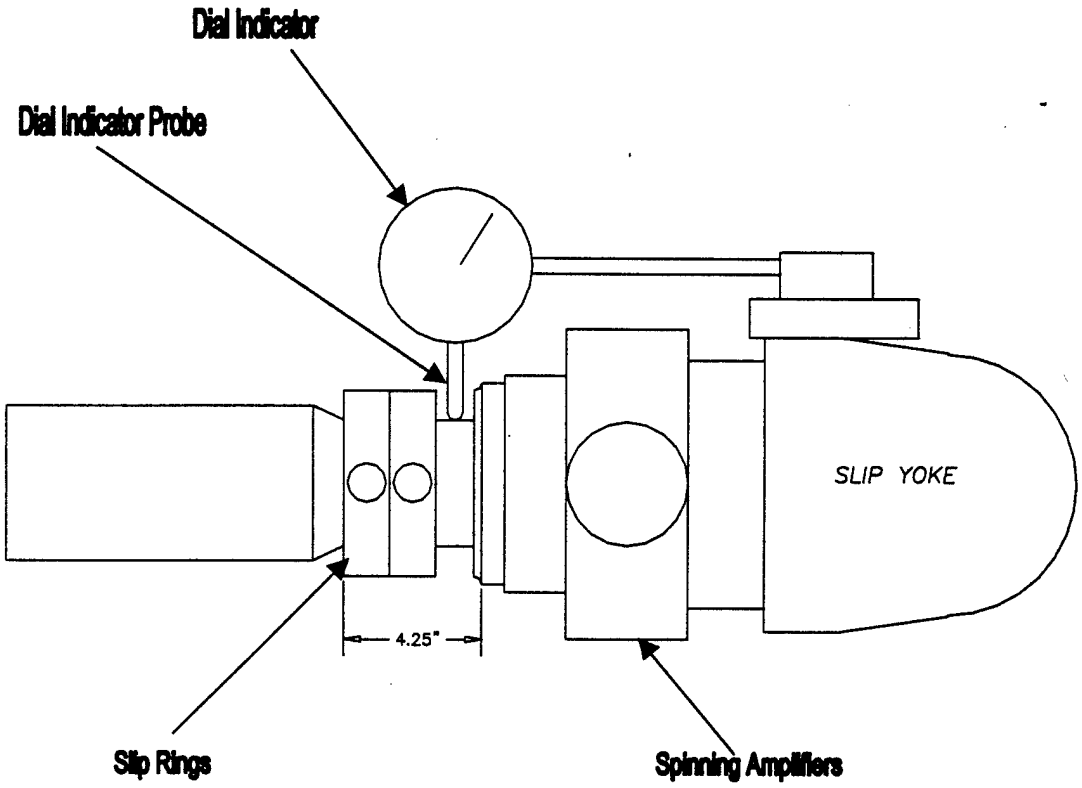

The slip yoke was lifted and a total displacment range of 0.007" as indicated by the dial indicator resulted.

APPENDIX H

SIMPLIFIED MECHANICAL MODEL, by Dr. John F. Martin, Michigan State University

(Appendix H of this report was authored by Dr. Martin as an independent consultant to TACOM)

Introduction

To quickly estimate dynamics and strength parameters associated with the driveline of the LMTV truck, a simple model was developed that could give advanced direction to the project. This model was kept simple enough so that a hand calculator or a short computer program could be used to determine values of natural frequency, stress, and strain in the flywheel housing and driveshaft. This model was intended to compliment the DADS computer based models that were under development by Michigan Scientific Corporation.

Using only very simple mechanics relations, the dynamic response and strength of the LMTV driveline were modeled. All components except the flywheel housing were assumed to be rigid bodies. Geometrical offsets in the driveshaft were input in the slip spline and universal joints along with an offset moment weight.

Summary

Basic dynamics and vibration theory were successfully employed to formulate a limited model of the overall mechanical behavior and durability of the driveline for the LMTV truck. Dynamic response was modeled with a one-degree-of-freedom, two-dimensional system consisting of rigid bodies connected to elastic springs that represent the stiffness of the flywheel housing. This model confirmed that a stiffened and strengthened flywheel housing no longer behaved as a major vibrational hinge in the system. Forces produced from the driveshaft were determined using basic trigonometric and dynamics relations. Hinging of the spline and looseness in the universal joints were inputs to the trigonometric relations.

Powerpack Model

The engine, transmission, transfer case, and flywheel housing were modeled as a simple dynamic system. Figure H.1 shows the chosen configuration. The engine, transmission, and transfer case were represented as rigid bodies: the engine as m_1 and the transmission/transfer case as m_2. The flywheel housing was represented by two springs that pivot about pin connections A and B as shown. Pin A represents the engine mounts and pin B represents the center of the mounting beam that connects to the flywheel housing and the transmission. Geometry, mass, and mass moments of inertia properties used were those available at the time.

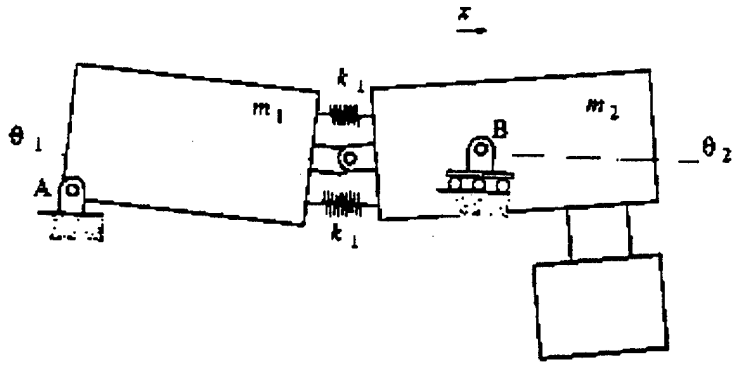

Figure H.1 Simple dynamic model configuration

APPENDIX H

Note that the engine is pin-jointed at A and the transmission/transfer case is pin-jointed at B with the freedom to move laterally. The powerpack is represented by a one-dimensional equation of motion.

$$\ddot{\theta}_1 + (9.72\times10^{-4})k_1\theta_1 = 0 \qquad (1)$$

where: $\ddot{\theta}_1$ = angular acceleration
θ_1 = angular rotation
k_1 = spring stiffness

This results in the following equation for the natural frequency.

$$\omega_n = \sqrt{9.72\times10^{-4}k_1} \qquad (2)$$

where: ω_n = natural frequency

Equation (1) can be used to determine linear accelerations anywhere in the system including the yoke connection on the transfer case. Equation (2) can be used to estimate the loads on the end of the transfer case. This interaction will be explained below.

Driveshaft Model

The driveshaft assembly was modeled as two right triangles placed back to back. The peaks of these triangles were located at the hinge caused by the spline coupling, see figure H.2. The long portion of the driveshaft was simulated with four equal masses (each one fourth of the total mass) that were evenly spaced. Equation (3) gives transverse forces, F_t, produced by each of these masses.

$$F_t = mr\omega^2 \qquad (3)$$

where: m = mass
r = offset
ω = angular velocity

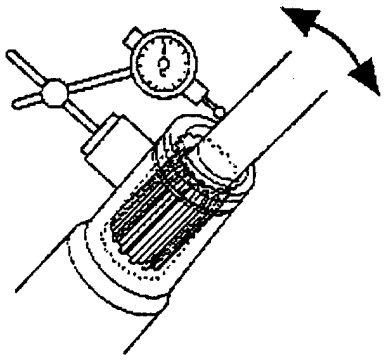

Figure H.2 Spline coupling

APPENDIX H

Equation (3) demonstrates the importance of vehicle speed as related to the forces produced by the driveshaft on the driveline system. The forces in the driveline increase as the square of rotational speed of the driveshaft and thus also as the square of vehicle speed.

Strength and Reliability Analysis of Flywheel Housing

Load and deformation behavior of the flywheel housing was modeled using strength of materials equations. The outer portion of the flywheel housing was treated as a hollow circular beam. The flat vertical portion of the housing where the transmission was bolted on was treated as a thin flat circular plate with a central rigid plug to produce the forces produced by the engine. These two relationships were combined to satisfy the continuity condition between the circular beam and plate. Assumptions were needed to formulate equations (4) and (5) below, however, these relationships proved to correlate well with experimental data.

$$\frac{1}{k_f} = \frac{1}{E}\left[\frac{0.20}{t} + k_1 \frac{82}{h^2}\right] \tag{4}$$

where: k_f = stiffness of flywheel housing

E = elastic modulus

t = average thickness of flat section

h = average thickness of circular section

$$\sigma_{max} = \frac{9.6 \times 10^{-3} M}{h^2} \tag{5}$$

where: M = bending moment

It can be seen in equation (4) that the parameter h (a squared parameter) is a significant input to this equation. Equation (5) gives the maximum stress in the thin vertical plate.

Strength and Reliability Analysis of Driveline

Stress and strains in the flywheel housing, along with g-loads anywhere on the engine, transmission, or transfer case can be determined. Once the stiffness of the flywheel housing has been calculated (equation 4), angular accelerations (equation 1) and natural frequencies (equation 2) can also be calculated. Cyclic forces from the rear driveshaft can independently be determined from trigonometric analysis and the centrifugal force (equation 3). Finally, dynamic cyclic forces, F_d, are estimated using the approximation given in equation (6).

$$F_d = F_s \left[\frac{1}{1 - \left(\frac{\omega}{\omega_n} \right)^2} \right] \qquad (6)$$

where: F_s = static load

Once again treating the overall assembly as a static problem but using the dynamic force as calculated from equation (6), the forces and moment can be determined anywhere on the powerpack. Also, g-accelerations can be determined once the angular acceleration in equation (1) is calculated from a known rotation angle that can be estimated from strength of materials principles.